CHAPTER 1

INTRODUCTION

The characteristic differences in the male and female skeleton, known as sexual dimorphism, are the most effective and germane traits with which to determine skeletal sex (Bass1995; Camacho *et al.* 1993; Dibennardo and Taylor 1983; Garn *et al.* 1970; McCormick and Stewart 1983; Navani *et al.* 1970; Tagaya 1989; Tarlie and Repetto 1986; White and Folkens 2000). Differences between males and females manifest themselves in numerous arrangements throughout both the axial and appendicular skeleton (Holman and Bennet 1991). Visual characteristics and osteometry both provide accepted methods for sex determination of unidentified skeletal remains. Non-metric (visual) determination is the use of morphological traits that establish whether a skeletal element is female or male, due to sexual dimorphism. For example, when researchers recover remains that include an intact cranium and pelvis, visual morphological interpretation is quite accurate for assigning a specific sex to the remains. Visual attributes of the cranium and the os coxae are the most accurate methods for determining sex from the skeleton, and continue to be the most appropriate and precise methods when these skeletal elements are available for analysis (De Villers 1968; Loth and Henneberg 1996; Phenice 1969; Steyn and Iscan 1998; Washburn 1948; Wescott and Moore-Jansen 2001). Quantitative (metric) analysis uses skeletal measurements from a known population to provide the same answer; in this case, the sex of the individual element examined (Evans 1976; Georgia *et al.* 1982; Grabiner 1989; Harper *et al.* 1984; Macho 1990; Mall *et al.* 2001; Pfeiffer and Zehr 1996; Richman *et al.* 1979; Steyn and Iscan 1999).

The ability to determine sex from long bones is important as well, and is utilized consistently when cranial and pelvic bones are absent or fragmentary (France 1998; Steele and Bramblett 1988; Woodard 1962). Because many of the

methods to determine skeletal sex are used in a medico-legal arena, (i.e., forensic anthropology), the use of proper techniques to achieve accurate results are paramount. Forensic anthropology is greatly impacted by new and more useful techniques in establishing individualizing characteristics of unknown skeletonized remains. Identification of skeletal remains is largely determined by the accuracy of the techniques used. Researchers have continually searched for more comprehensive, precise and accurate methods of sex determination to augment existing practices. Combined, the use of quantitative and qualitative analysis plays a significant role in determining skeletal sex.

Historically, numerous challenges have presented themselves as researchers continue to determine the most applicable methods to predict skeletal sex from postcranial long bones with precision and accuracy (Albanese *et al.* 2005; Allen *et al.* 1987; Bidmos 2006; Sakaue 2004; Steyn and Iscan 1997). The lack of grossly distinct sexual dimorphism in humans can make qualitative analysis difficult. Intra-population variation poses challenges which center around the principle component of size in quantitative analysis (Asala 2001; Asala *et al.* 1998; Purkait and Chandra 2004). Different populations exhibit different skeletal dimensions, to which accurate formulae must be applied. To compound the problem, fragmentary and incomplete remains are difficult to measure. Therefore, researchers have continually sought accurate methods of sexing skeletal elements when the pelvis and cranium are absent and only more robust postcranial elements remain (Case and Ross 2007; Introna *et al.* 1998; Özer *et al.* 2006; Pons 1955; Sorg and Haglund 1997). These methods are particularly desirable for long bones, which may not have distinctly different characteristics indicating sex, but tend to survive in the field quite well. So far, several methods of sex determination from skeletal elements other than the cranium and pelvis are gaining merit. The structure of the lower limb bones (femur, tibia and fibula) and their sexually dimorphic traits have been the subject of study and produced promising results (Martin and Atkinson 1977; Ruff 1987). Thus, these

sexually dimorphic characteristics would be considered extremely valuable in the realm of medico-legal death investigations, in archaeology, and in biological anthropology research.

In addition to quantitative and qualitative methods of determining sex, geometric morphometrics allows for a detailed shape analysis based on the use of comparable landmarks of certain skeletal elements (Adams 1999; Bookstein 1986, 1991, 1996; Kendall 1981; Rohlf and Marcus 1993; Siegel and Benson 1982). This relatively new method places numerical values on shapes and has been shown to be quite useful in the determination of sex using discrete areas of skeletal morphology such as the greater sciatic notch and the human orbit (Pretorius *et al.* 2006; Steyn *et al.* 2004). The lack of grossly distinct sexual dimorphism in humans can make visual assessment of skeletal elements challenging, and problems with the classification of visual traits (e.g., symmetrical, intermediate, asymmetrical) continue to be a dilemma not yet resolved (Ferson *et al.* 1985). Thus, geometric morphometric analysis appears to be at the forefront of techniques that combine the accuracy and repeatability of metrics with the form-and-contour analysis of visual assessment.

The study of skeletal differences between males and females has rarely taken into account the physical change in hard tissue characteristics with the onset of advanced age. In order to observe sexual dimorphism in the adult human skeleton, knowledge must be gained with regard to the development of these sexually dimorphic traits and the changes which they may undergo during life. Anatomical change through human developmental processes and successive degenerative modification pose a serious challenge when diagnosing the sex of an unknown individual of considerable age. Many fields (orthopaedics and geriatrics for example) have outlined the process of age changes to bone, as well as the extent and location of these changes (Grynpas 1993; Genant *et al.* 2007; Parfitt 1997; Rogers 1982; Ruff 2000; Ruff and Hayes 1982; Schnitzler *et al.* 1990; Schnitzler and Mesquita 1998; Stout and Robling 2000). No studies, however, have made diagnostic

determinations regarding how skeletal morphology of the aged affects the way osteologists and physical anthropologists use and perhaps adjust their identification techniques. The use of non-metric and metric techniques may become more accurate based on a clear increase in sexual dimorphism with age; on the contrary, if sexual dimorphism decreases with age, the standard course of analyses may lead to an erroneous conclusion regarding the sex of the individual in question. Little is known about the visual and metric transformation of hard tissue with age, let alone how this would presumably effect a researcher's determination of sex from the skeleton. Does sexual dimorphism in hard tissue, in fact, decrease or increase with advancing age?

The aim of this study is thus to establish whether sexual dimorphism changes with age. This issue would be addressed by using three levels of procedural analyses. It would firstly elucidate whether or not metric traits are altered with the advancement of age; it would also determine if visual assessments using archetypal techniques are more or less accurate as age increases; and thirdly, whether or not geometric morphometrics using homologous landmarks differ from younger to older individuals when attempting to determine sex.

CHAPTER 2

LITERATURE REVIEW

The purpose of this chapter is to discuss the development and degeneration of the skeletal system as it pertains to sexual dimorphism. Sexual dimorphism, the anatomical and morphological differences between males and females, is used consistently to draw conclusions pertaining to the eventual identification of an unknown individual. The inherent size and physical variation between males and females makes sexual dimorphism a powerful tool in assessing skeletal sex. Changes with age, and how these changes affected the characteristics of long bone morphology in males and females were the motivation for this research. However, even taking into consideration the relative size differences between males and females, difficulties can occur. Sexual dimorphism in humans can show enough variation among populations such that the determination of sex can become challenging when morphological features are ambiguous (Kennedy 1995). Therefore, a review of how sexual dimorphism develops in humans, how it manifests itself in developing and mature individuals, and how it potentially is modified in the aged indicates where most research has been concentrated, and where research has yet to accomplish comprehensive results.

Information in this chapter covers the developing skeleton and how the degree of sexual dimorphism changes as humans age, as well as studies that have been instrumental in documenting these changes. Additionally, the location of these changes, the type of bone that is modified with age, and the actual mechanisms that cause changes in bone with the advancement of age are assessed. Since this study employed three methods of determining sex from the human skeleton; metric quantitative techniques, non-metric visual techniques, and geometric morphometric techniques, these methods, and their relative success for the determination of sex

are discussed. Because this specific study only involves the postcranial skeleton, focus will be directed on hard tissue morphology as it relates to long bones and the pelvis, and not the cranium. References to skeletal material will be in the context of observing characteristics of postcranial morphology.

2.1

Manifestation of sexual dimorphism in the human skeleton

Studies in developmental changes and hard tissue growth before and after puberty have been extensive (e.g., Bushang *et al.* 1983; Buckberry and Chamberlain 2002; Cummings and Black 1995; Evans 1976a, b; Garnero and Delmas 1998; Garn 1972; Imrie and Wyburn 1958; Iscan *et al.* 1985; Lee *et al.* 1996; Meuller *et al.* 1966; Recker *et al.* 1992; Steele and Bramblett 1988; Steiger *et al.* 1992; Weaver and Chalmers 1966a, b; Young and Heath 2000). Bone development and growth occurs by the incremental replacement of cartilaginous material (endochondral ossification) or the direct replacement of mesenchyme (intramembranous ossification). Heath and Young (2000) described the long bones, vertebrae, pelvis and bones of the base of the skull as being preceded by cartilage, thus formed through endochondral ossification. Long bones are well established to have an outer matrix of cortical bone, which provides rigidity and strength, and a longitudinally located medullary cavity of thin interconnecting bone trabeculae, in which haemopoietic bone marrow is formed and stored. The shape, orientation and thickness of bone and bony elements are dependent upon the functions and stresses to which the particular bone is exposed. Weight-bearing bones (such as vertebrae and femoral necks) may exhibit numerous thick intersecting trabeculae, while very few trabeculae are found in non-weight-bearing cortex of the rib. These general characteristics of bone are homogenous between developing male and females, and originate from a common, primitive, mesenchymal cell type. Pre-adolescent males and females do not appear

to exhibit differing skeletal attributes on a microscopic or histological level (Garn 1972).

It has been established, however, that males and females begin to skeletally diverge into separate anatomical entities after birth (Bruzek and Soustal 1984; Coleman 1969; Hoppa 1992; Loth and Henneberg 2001; Miles and Bulman 1995; Reynolds 1945). Sexual dimorphism, in its most fundamental application, may begin to develop before puberty (Merchan and Ubelaker 1977; Moerman 1982 a and b, 1992; Reynolds 1947; Roche and Davila 1972; Tanner 1962; Tanner *et al*. 1976). Most of the sexually dimorphic characteristics that were the focus of this study are absent in the pre-adolescent bones of humans, and develop only as a result of the adolescent growth spurt which occurs during puberty. However, there are several indications in other skeletal locations besides the tubular long bones that may offer evidence of sexual dimorphism in the developing skeleton.

Research on the prepubescent innominate bone by Imrie and Wyburn (1958) and Schutowski (1987) suggest that morphological differences in this sex-specific skeletal element do exist, but many of these differences are either subtle or not inherently obvious until full maturation of the human skeleton. Other studies conducted on the pelvis (Humphrey 1998; Moerman 1981; Rissech and Malgosa 1997) concluded that after the metamorphosis of the pelvis to male and female forms at puberty, hard tissue in the region exhibits little change with regard to sexual dimorphism. When attempting age estimation on the auricular surface of relatively young individuals, Buckberry and Chamberlain (2002) found that rates of skeletal development, remodeling and degeneration in the pelvis (from which most methods of adult sex and age estimation are derived) could be highly variable between individuals and populations. They also found, surprisingly, that after the initial development of the adult os coxae and the primary growth surge during puberty, the bones of the pelvis remain relatively static in morphology between males and

females. In other words, a lack of systematic variation in the rate of aging between the sexes was observed.

Although this study does not involve cranial morphology, development of the cranium and its possible sexual dimorphism in children has been researched (Molleson *et al.* 1998; Newman and Meredith 1956; Scheuer and Black 2004; Schutkowski 1993; Walker 1972). Studies involving prenatal cranial development do not discern between males and females in their research, leading to the idea that differences between the two sexes are minimal in utero (Goldberg *et al.* 2005; Jeffery and Spoor 2001). Cranial bone and its properties in regard to tensile strength and bone failure rates due to trauma do not indicate a distinction between males and females, either. Studies of infant cranial bone focus primarily on the strain capacity, fusion rates for developmental purposes, and potential consequences of infant cranial trauma but again do not distinguish a difference between male and female infant cranial properties (Coats and Margulies 2006; Kriewall 1982; Margulies and Thibault 2000; Peterson and Dechow 2002, 2003; Sun *et al.* 2004;).

Continual ossification and development of all cranial elements continues after birth, and exhibits variable rates of growth and maturation. Craniofacial features are used consistently to assess sexual dimorphism in the skull of adults, and most craniofacial growth takes place before puberty (Scheuer and Black 2004). The beginnings of sexual dimorphism, then, is considered evident in this region of the cranium and may even be assessed to a certain level of accuracy in infants, but does not become inherently apparent in juveniles until after skeletal changes begin at puberty (Buschang *et al.*, 1983, 1986; Humphrey 1998; Hunter and Garn 1972; Loth and Henneberg 2001; Molleson *et al.* 1998; Newman and Meredith 1956; Schutkowski 1993; Walker and Kowalski 1972). Growth rates between boys and girls are expected to be different, and sexual dimorphism in the craniofacial region may be observed and calculated (Scheuer and Black 2004).

Males and females do not only differ in the rates in which their pelves and crania develop (and in what morphological direction, i.e. tendency towards robusticity in males or maintenance of infantile features in females), but in long bone maturation as well. Male and female rates of long bone maturation are known to be different. Cross-sectional studies performed on age and hard tissue progression towards adulthood indicated that during pubertal development, major differences between growing males and females were observed in bone mass progress according to sex and skeletal site (Bonjour *et al.* 1991). Specifically, male bone mass at different skeletal sites (lumbar vertebrae, femoral neck) continued to increase substantially between 15-18 years, but skeletal mass growth in females appeared to dramatically slow down at these same sites during the same age range. Subsequently, females showed a dramatic reduction in general bone mass growth after 15 years.

Garn (1972) investigated the relative rates of bone gain at the outer periosteal surface and the proportional rates of bone loss/ gain/ loss at the inner endosteal bone surface, which determined the gross size of the bone in addition to the amount of cortical bone within the anatomical bony element. These studies were performed throughout progressing age stages. Garn constructed the phases of bone resorption primarily at the endosteal surface of long bones and concluded that the majority of bone remodeling occurs during the 4^{th} (adolescent-to-adult) phase and 5^{th} (adult) phase of endosteal surface resorption. He also recognized a sexually dimorphic component to lifelong bone apposition at the subperiosteal surface and concluded that females exhibited a resorptive phase demonstrably larger than males that reduced skeletal mass after adolescent developmental stages were complete. This showed that dynamic processes were occurring in adolescent bones that were different between males and females, even at an early age. These dynamic processes continued to be divergent between the sexes throughout life.

Bone mass modification, remodelling, and transformation in young males and females have always shown net gains in the density of cortical bone and in the

overall density provided by active osteoblasts within both the endosteal and periosteal envelopes (Thompson 1980). Bone development in both males and females is truly a dynamic process, and the incremental addition of bone in early life can certainly play a role with regard to the way individuals change as they begin to age, skeletally, in the 3rd decade of life and beyond.

Based on the dynamic and extraordinary changes that occur in the developmental cycle of bone formation and maintenance specifically in the female skeletal system, females have been studied consistently for the last few decades, and studies on the maturation of the female skeleton have a wealth of information on which to base fundamental principles of bone gain and foundational bone density (Georgopoulos *et al.* 2001; Levine 1972; Onat and Iseri 1995; Singer and Kimura 1981; Vidulich *et al.* 2006). In general, women past the age of puberty tend to gain bone mass through the 3rd decade of life, and may even continue to gain bone if calcium supplements and exercise are introduced (Recker *et al.* 1992). In addition, specific emphasis on such features as cortical bone thickness and bone mineral density in healthy adults has provided a gauge with which to determine maturation rates and subsequent degenerative processes (Dickenson *et al.* 1981; Epker *et al.* 1965; Gotfredsen *et al.* 1987; Hui *et al.* 1985; Jowsey 1960; Matkovic *et al.* 1990; Woodard 1962).

2.2

Other factors that influence sexual dimorphism in a population

Many unique and vigorous influences on hard tissue play roles in its early development, its maturation, its variation into adulthood and its degenerative characteristics. These influences vary greatly and offer different aspects of morphological variation.

Structural characteristics in the skeleton upon maturation and its "level" of sexual dimorphism correlate often with behavioural factors (Chesnut 1993). Specifically, it has been proven that without weight bearing exercises performed consistently to strengthen hard tissue (i.e., mechanical loading or gravitational force exercises), bone mass loss will occur at axial and appendicular skeletal sites (Skedros *et al.* 2004). Weight-bearing processes that occur in the realm of occupational functions were found to strengthen muscle attachments and articular joint surfaces even to the point of modifying morphology in bone's adaptive processes. Thus, mechanical loading and behavioural stressors play a distinct role in factors influencing bone mass and structural morphology (Beck *et al.* 1992, 2000; Burr and Martin 1983; Chavassieux *et al.* 2007; Compston *et al.* 2007; Han *et al.* 1997; Maalouf *et al.* 2007; Seeman 2003; Szulc *et al.* 2006). Thus, if behavioural practices are distinctive between the sexes this can play a role in the sexually dimorphic nature of bone in males and females. Behavioural practices have been seen to be very distinct between populations and cultures. Males and females respectively play different roles in their societal environments, thus they are subjected to different physiological and biomechanical stressors. These influences have residual effects on hard tissue (Anderson 1998; Beck *et al.* 1990, 1992; Ruff *et al.* 2006; Taitz 1998).

In addition to behavioural aspects influencing bone mass and hard tissue density, environmental, nutritional and socioeconomic issues have also been shown to play a vital role in skeletal structure (Angel *et al.* 1987; Macho 1990; McVeigh *et al.* 2004; Nelson *et al.* 2004; Ruff 1987; Stini 1969; Thompson 1980). Macho (1990) determined that different living conditions and/ or nutritional availability affected bones in complex ways of which linear growth was only one aspect. As nutrition improved in the African and European populations studied, so did sexual dimorphic characteristics as well as stature. Based on this discrepancy in size and the question of stature as an indicator for living conditions, Macho concluded that relative size

variations, i.e., shape, discriminated more clearly between the sexes than did observable size when nutritional stressors were recognized as a factor. It was also concluded that when the level of nutrition improves, the amount of sexual dimorphism in stature increases (Tobias 1975; Tobias and Netscher 1977).

Other nutritional studies have focused on the rate of calcium absorption and the direct effects of reduced calcium assimilation in the body (Devine *et al.* 2004; Heaney *et al.* 1982). Heaney's study concluded that as a decrease in the intestinal calcium absorption efficiency and renal calcium conservation occurred, the medullary cavities of long bones expanded due to loss of mineral density within the endosteal-trabecular envelope. The study also determined that the average elderly person is in negative calcium balance; this fact coupled with factors such as decreased mechanical loading of the skeleton must figure prominently in age-related bone loss throughout the entire skeleton.

Behavioural and nutritional issues, among other factors, take part in skeletal differences between men and women. Perhaps two of the most important factors in sexual dimorphism are those that determine the sex of an individual itself (genetics) and those that inevitably cause maturation changes to occur (hormones). Both hormones and genetics are known to influence skeletal attributes (Ebeling *et al.* 1998; Kelly *et al.* 1990; Manning *et al.* 1992; Pollitzer and Anderson 1989).

Naturally-occurring hormones are, in fact, the basis for all bone development and maturation (Young and Heath 2000). Specifically, bone development is controlled by growth hormone, thyroid hormone, and the sex hormones. In addition, synthetic hormones used in the medical treatments of some disease processes also influence subsequent bone mass and hard tissue density. For example, the study Ebeling *et al.* performed (1998) determined that long-term inhaled or oral glucocorticoid administration for asthmatics lowered bone mineral density in both men and women. In addition to the loss of critical bone density, which acts to prevent fractures, glucocorticoids reduced bone formation in the presence of ongoing

bone resorption, which contributed directly to ultimate bone loss in asthmatics. These findings were mirrored by that of Jee *et al.* (1970), which confirmed that hormones such as corticosteroids were relevant to the decay of osseous tissues and reduced bone volume. Going further, Jee *et al.* deduced that the effect of corticosteroids was dose- and time-dependent, in which high doses of the steroid suppressed bone resorption and low doses stimulated bone resorption; corticosteroids thus act upon bone cells by directly inhibiting precursor cell proliferation.

Studies focused on genetic markers for bone loss and resorption provide significant evidence that bone turnover markers are of value in investigating the pathogenesis and treatment of bone loss in young and old (Garn *et al.* 1966; Looker *et al.* 2000). Genetics plays a significant role in the bone mass of an individual, and the genetic markers for that role can be studied and identified. These markers can lead to information with regard to specific bone gain in the developing skeleton of a young adult or subsequent bone loss and degenerative processes in the elderly. Genetic bone resorption markers appeared to be associated with increased fracture risk in elderly women, while there is less of a correlation between bone formation markers and fracture risk. Biochemical markers appeared to be valuable tools in the research of metabolic bone gain and loss, which in turn is applicable to bone density and mass.

The types of stresses that are applied to osseous tissue, which determines how dense and compact the existing trabeculae should be in a given area of stress, can also influence initial bone mass in the human skeleton. The tensile strength of osseous tissue functions as one of the main components of the mechanical properties of bone, especially as the human skeleton ages. Stresses to the tensile property of bone increase the risk of fractures, subsequent wound response, and compensatory actions by the injured and thus inherent biomechanical substitution occurs, possibly changing the anatomy of the injured element (Evans 1976). All of

these aspects determine the variance of hard tissue morphology from puberty to advanced age. Some of these changes manifest themselves in quantifiable variables, and others appear to exhibit conditions that may be best visualized other than measured.

2.3

Previous research in age-related changes in sexual dimorphism

Those interested in osteoporosis and its effects on the elderly population performed the majority of past research done in this area of skeletal anatomy (e.g., Adebajo *et al.* 1990; Aspray *et al.* 1996; Grynpas 1993; Maalouf *et al.* 2007; Ruff and Hayes 1982; Schnitzler 1993; Simmons 1985; Szulc *et al.* 2006; Wallin 1994) . Thus, different disciplines of expertise were the sources of much of the literature defined in this section. However, previous studies in these disciplines do illuminate the histological, microscopic and macroscopic modification found in bone of advanced age, thus they were considered valuable to utilize.

Bone loss and bone modification are multi-faceted processes of skeletal maturation, maintenance, and degeneration. These processes affect all types and categories of bone, from exterior cortical surfaces to the underlying matrix of the medullary cavity. Bone modification as the human skeleton ages not only affects the periosteal surface of the long bones, but also inflicts a net loss of bone mineralization within the cortical bone surface as well as the cortical endosteal surface (Epker 1965; Frost 1963; Gotfredsen *et al.* 1987; Jowsey 1960; Ruff 1987; Thompson 1980; Woodard 1962). Studies have focused primarily on the net bone loss of individuals (both male and female) of advanced age and show that this loss takes place primarily from the cortical-endosteal surface (Aloia *et al.* 1985; Deakins and Burt 1944; Evans 1976; Nilas *et al.* 1988). This type of loss was then observed to cause an expansion

of the medullary cavity while simultaneously exhibiting cortical bone thinning (Heaney *et al.* 1989; Leiel *et al.* 1988; Martin and Atkinson 1977). This type of modification typically resulted in an expansion of tubular bone circumference *within* the medullary cavity, but not necessarily in the corresponding outer cortical "shell" or envelope. Alternative studies by the Scientific Advisory Board of the National Osteoporosis Foundation (1988) discovered that age-related bone loss in the shafts of long bones is partially compensated for biomechanically by remodelling to increase the shaft diameter. This served as a response to increase resistance to bending and torsion in the limb shafts of both men and women. This compensation process was found to be at not only the long bone shafts, but also in the articular junction of joints.

Further distinctions between males and females in the compensatory reaction of thinning cortical bone and increased bone porosity were found, which contrast the results of the National Osteoporosis Foundation. Female skeletal changes occurred most dramatically at the onset and after menopause, where bone remodelling became unbalanced and resulted in bone loss at each remodelling site (i.e., articular joint surfaces). In addition, an increase in bone turnover sites resulted in an accelerated bone loss throughout the entire female skeleton (Cummings *et al.* 1990; Herd *et al.* 1992; Herrin 2001).

The location of remodelling, which represented skeletal tissue undergoing modification and therefore becoming structurally ineffective, increased in females with age and was observed in greater quantities in cancellous bone as opposed to cortical bone. These changes manifested themselves in greater microporosity, a decrease in bone mineral density, and the onset of frequent osteoporotic fractures at sites such as the femoral neck and the vertebral bodies (Cummings *et al.* 1985; Cummings *et al.* 2000; Dickenson *et al.* 1981; Evers *et al.* 1985; Hurxthal *et al.* 1969; Kanis and McCloskey 1993; Orwoll *et al.* 1996; Steiger *et al.* 1992; Thompson 1979). Riggs *et al.* (1982) categorized this bone loss further into "postmenopausal osteoporosis", characterized by excessive and disproportionate trabecular bone loss

associated mainly with vertebral fractures; and "senile osteoporosis", a more general term, which is characterized by a proportionate bone loss in both cortical and cancellous bone.

Males, conversely, showed an increase in bone porosity with age but also exhibited compensatory structural strength that did not occur in females. This mechanism indicated a physiological adaptation resulting in a difference between males and females and their varying deficit of bone surface remodelling that is independent of internal remodelling (Martin and Atkinson 1977). Age-related bone change in males was also linked explicitly to unique hormonal changes related to prostate health, including treatments for cancer and other age- and gender-related therapeutic management (Bilezikian 1999; Daniell 1997; Eastel *et al.* 1998; Finkelstein *et al.* 1987; Grasswick and Bradford 2003; Ross and Small 2002; Thiebaud *et al.* 1996; Vasireddy and Swinson 2001).

Various studies from different biological groups found throughout the world give further details about the unique characteristics in patterns of bone modification with age. Spinal density in females from Japan and India with low calcium intake decreases dramatically with age, in contrast to British and American populations (Nordin 1966). Several studies have indicated that higher bone mineral densities in African American subjects were a reasonable explanation for differential fracture rates when contrasted with American white females (Aldridge 2005; Garn *et al.* 1969; Garn 1972). Osteoporosis was seen with less frequency in African American females as well, and Trotter *et al.* (1960) determined that bone density is not only sex-specific (male osseous material is denser than female osseous material) but population-specific as well (African Americans exhibited greater bone density as did American whites). Orwoll *et al.* (1996) were forced to remove African American women from their axial bone mass and fracture study based on the low incidence of hip fractures. A Native American sample of three geographic groups were seen to parallel bone loss studies conducted on American white female samples, with overall

loss of cortical bone amounting to two to three times that of males (Ericksen 1976). Finally, mineral density levels in Eskimo tibiae were found to again follow a classic model of cortical and cancellous bone loss, with male bone density measurements exceeding those of females as age progressed and female bone mineral density declining with age (Martin *et al.* 1985). In studies to date, even when focused on specific geographical groups, bone loss is seen with advancing age in both sexes and in all biological affiliations.

Although research has focused primarily on the net periosteal and endosteal bone loss of individuals with the onset of age, others report the surprising increase of total diameter of long bones due to a periosteal bone gain, and the continued positive periosteal bone balance (indicating continued periosteal bone formation) after the age of 65 years (Jowsey 1960; Smith and Walker 1964). Smith and Walker (1964) specifically showed evidence of the mean periosteal femoral diameter increasing as cortical thickness declined. Since the cortical area was enlarged, periosteal accumulation exceeded endosteal resorption, meaning a net bone gain was found due to periosteal bone activity that superseded the endosteal bone loss. This same result was seen in humeral dimensions from Rother *et al.*'s study (1977) where quantitative overlap was found between the sexes. Subsequently, it was concluded that humeri showed a decrease in sexual dimorphism with age.

Evans (1976) reported that as age increased in the human skeleton, the incidence of fractures increased for two reasons: first, because older individuals exhibit less bone density (a quantitative difference) and because the osseous material of older individuals is structurally weaker than that of younger individuals (a qualitative difference). An increase in osteon numbers is also found in older individuals, which subsequently increased the amount of cement lines around osteons in a given area. Thompson confirmed this observation in his 1979 study of age-at-death determination by osteon count. Other researchers who study age-at-death with bone histology methods have mirrored his conclusions (Ortner 1975;

Young and Heath 2000). The increase in osteons led to an increase in structural porosity (due to increased canals, lacunae, and canaliculi) and created sites more prone to microfractures based on fracture patterns around the cement lines surrounding osteons. The 1) increase in porotic spaces of bone and 2) increased numbers of osteons per millimetre squared decreased the amount of hard tissue available for force resistance or load-bearing strength. These tensile stresses resulted in microfractures, which subsequently resulted in more active bone remodelling sites, which finally manifested in an increase in bone surface area and dimension.

Nilas *et al.* (1988) advanced this theory by reporting the increased bone width at two forearm sites in females while originally attempting to observe bone loss. In addition, Linday *et al.* (1978) determined that estrogen replacement therapy in osteoporotic women prevented further bone loss in postmenopausal women and in fact modestly increased bone mass if estrogen treatment had been delayed for several years.

Irregular bones such as the structure of the hyoid bone have been examined as well, and showed similar results in cumulative bone gain to their surfaces with age, resulting in larger bone mass and increased asymmetry (Miller *et al.* 1998). These areas of aggregate bone change appear contradictory (or in the very least, contrasting) from one study to another, and have been examined in detail to understand the total changes affected upon the skeleton. In general, females appear to be either maintaining their size or becoming larger in skeletal dimensions, which may be a reason for the reduction in sexual dimorphism with age between the sexes in any given population.

Walker (1995) provided a comprehensive study of an English population that elucidated the challenge of age-related changes in bone when studying sexual dimorphism. Because decreased bone density in women was highly correlated to the degradation of skeletal material in Walker's cemetery sample, os coxae could not

be utilized on a large scale to confirm sex classification. Disintegration of the greater sciatic notch and other pelvic features lead researchers to categorize sex from craniofacial features; these features ultimately suggested that post-menopausal females contributed to the apparent excess of males in the skeletal collection due to misclassification based on supraorbital robusticity. Walker cautioned that overlooking these age changes in female postmenopausal cranial morphology could introduce significant biases regarding the determination of sex in mortality profiles (and forensic analyses) based on poorly preserved skeletal collections or samples.

In conjunction with this was Walker's study of greater sciatic notch morphology (2005), and its determination that there was a greater tendency for male sciatic notch morphology to shift in a masculine direction with increased age, resulting in greater sexual dimorphism. Both young males and females tended to have more feminine morphology than did older individuals. This feminine morphology appeared more prevalent in young males, and thus the shift in a more "male-like" morphology with age was quite dramatic.

The extensive changes documented in past research summarized here may suggest that perhaps these modifications appear in bone concurrently. The human skeleton changes dynamically with the onset of age after puberty. These changes manifest themselves in both the negative and positive; bone is both lost and gained depending on the skeletal site, various biological factors, and sex of the individual. Anthropological analyses on skeletal material have been extensive and comprehensive in documenting morphology of the skeleton. The discipline of anthropology is also established in its extensive array of research performed on the intricacies of sexual dimorphism and how to categorize skeletal sex. While performing initial inquiries into the subject, however, all disciplines appeared to be lacking in documentation regarding how each effects each other; how hard tissue anatomy changes with the onset of advanced age, and if the differences between young and old individuals is great enough to note, and large enough to quantify. It is

this discrepancy between posing the query and finding the answer that outlines the need to understand the extent of these changes, and their physical manifestation on elements used to make scientific determinations of sex.

Sexual dimorphism is known to be apparent in the human skeleton, but a review in how anthropologists determine sex from skeletal elements may aid in determining which elements are important and which ones could be susceptible to modification with age.

2.4

Non-metric techniques for determining sex in the postcranial skeleton

Researchers historically have used quantitative analysis on postcranial elements and discovered its benefits early on; however, most agreed that nothing could take the place of a visual assessment of specific skeletal element's characteristics by a trained and experienced analyst (Stewart 1954). Most of these visual techniques historically have been used on the cranial and pelvic regions, and not long bones. Although some researchers considered measurements to be more accurate than visual techniques, they continually argued that there are inherent limitations to measurements, "...namely, that they are poor descriptive agents and are subject to various kinds of error. As is all too well known to anthropometrics, an index tells nothing but the percental relationship of two linear dimensions; it tells nothing about the shapes of the parts included within the dimensions" (Stewart 1954). Many researchers concluded that measurements were no substitute for visual assessment by an experienced analyst who can quickly and effectively diagnose the sex of a skeleton (Hill 2000; Inman *et al.* 1944; Ubelaker and Volk 2002; van Dongen 1963; Walrath *et al.* 2003; Weiss 1972). For example, Van Dongen's research on the shoulder girdle and humeral element of Australian

Aborigines showed numerous applications of visual, non-metric assessment in order to discern males from females. Most of the specimens in this sample would have been misclassified as male based on metric techniques applied to epiphyseal long bones sites and shaft diameters.

The dominant factor in quantitative analysis for all populations is nearly always size, and its relationship to males versus females. When size is "removed" from the statistical analysis of sex, only descriptors are left to reveal differences between sexes and establish clear guidelines with regard to what constitutes male and female morphology. Visual characteristics and their meaning are inherent in anthropological research. Quantitative analysis depends solely on size differences to correctly assign sex, but this method fails where the sexes over lap (i.e., a large female or a small male).

Visual assessment offers an alternative by relying on descriptive features and observer experience to interpret the distinctive variation in shapes between male and female elements, and to come ultimately to an accurate conclusion (Wanek 2002). Specifically, visual assessment of the distal and posterior humerus uses several characteristics to determine skeletal sex, a technique that was developed by Rogers (1999). Physical characteristics of olecranon fossa shape, the angle of the medial epicondyle, the absence or presence of symmetrical borders between the trochlea and the capitulum, and the position of the medial epicondyle within the trochlear profile were all sexually dimorphic. These traits, which were tested on a Caucasian sample by Rogers and subsequently tested on numerous populations by Wanek (2002), were shown to be sexually dimorphic, and again provided another non-metric technique that focused on sexual dimorphism in sex determination.

Some non-metric visual techniques have been developed and tested innumerable times with the same results. These methods hold some of the most accurate and appropriate means by which to determine sex in the adult human skeleton. Specifically, a detailed description of pelvic traits has endured throughout

decades of anthropological research and continues to fill many of the canonical texts used by students, researchers and scholars alike (Bass 1995; Krogman 1962; Steele and Bramblett 1988; White 2000). Physical characteristics of visual pelvic morphology are conventionally based on shape, contour, angle, the relative width of a feature, or a combination of several morphological traits. Common physical characteristics of the pelvis, which appear as sexually dimorphic, are the width of the greater sciatic notch, the width and robusticity of the ischio-pubic ramus, the shape and width of the subpubic angle, and the contour of the subpubic concavity. All of these features show distinct differences between males and females, and have been documented extensively in their scope of accuracy in numerous biological populations.

Because these suites of features from both the humerus and pelvis have been established as accurate ways of assessing sexual dimorphism in the human skeleton, they were employed in this study as the characteristics in which to establish sex by non-metric, visual means.

2.5

Metric techniques for determining sex in the postcranial skeleton

Metric studies were brought about by a need to quantify traits identified by visual techniques. Sexual dimorphism in a classic sense illustrates the observable, physical characteristics that make males and females anatomically distinctive from one another. Many professional osteologists, physical anthropologists and anatomists rely on these characteristics in order to determine the fundamental, individualistic information from a skeleton. The postcranial skeleton continues to be a source of information in regard to determining skeletal sex because most long bones exhibit noticeable size differences (Borgognini Tarli and Repetto 1986).

Various researchers have studied the metric differences between males and females in the long bones of the upper limb (e.g., Jantz *et al.* 1994; France 1998; Grabiner 1989; Mall *et al.* 2001; Richman *et al.* 1979; Steyn and Iscan 1999), the lower limb (King *et al.* 1998; Martin and Atkinson 1977; Thompson 1980; Woodard 1962) and the pelvis (Phenice 1969; Steyn *et al.* 2004). Many of these studies focus on the dimensions of articular joint surfaces such as the humeral or femoral head, and distal epicondylar breadth. Several provided discriminant function formulae for the determination of sex for multiple population groups (Dibennardo and Taylor 1982; Giles and Klepinger 1998; Richman *et al.* 1979; Tagaya 1989). These measurements have now become standard, such that they are easily repeatable and reproducible by researchers.

In addition to epiphyseal measurements on long bones, the length of long bones, their diaphyseal diameters, and their circumferences have been the subject of diverse studies which span from anthropology to geriatric medicine (Evans 1976; Garn 1970; Georgia *et al.* 1982; Harper *et al.* 1984; Klepinger 2001; Leiel *et al.* 1988; Macho 1990; Pfeiffer and Zehr 1996; Stewart 1963; Stini 1969; Woodard 1962). These studies and their subsequent development of sex determination techniques focus on the principal size component of long bone shaft diameter discrepancies between males and females in the appendicular skeleton (King *et al.* 1998; Martin and Atkinson 1977; Thompson 1980; Woodard 1962). As expected, all these researchers found differences between males and females, with Chesnut (1993) observing additional linear correlations between the maintenance of bone mass and the implementation of weight-bearing exercises (mechanical loading) regarding to the shoulder girdle and elbow joint. Factors such as these (i.e., size components, weight-bearing differences) and the broad-spectrum differences in male and female anatomy make sexing methods of the postcranial skeleton quite robust and accurate when utilizing a known sexually dimorphic trait or suite of traits.

Most of these studies focus on the bimodally distributed metric differences between males and females, the variation of shaft diameters with age and osteoporotic degenerative changes, and the possibility of metric overlap between populations and/ or sexes. Metric studies concluded that males, regardless of population, are larger in size than their female counterparts (Takahasi and Frost 1965; Wiredu 1999). Articular surfaces and breadths are greater, shaft diameters are larger and tubular bone lengths are consistently longer in males than females. Since men are morphologically larger than women, quantitative analysis depends solely on these size differences to correctly assign sex. Thus long bone morphology and their unique attributes at epiphyseal junctions as well as shaft and length dimensions continue to be the focus of sexual dimorphism research.

2.6

Geometric morphometric techniques for determining sex from the postcranial skeleton

Morphometrics in biology has been utilized consistently for the past twenty years for species determination, developmental transformation, and sexually dimorphic variation between males and females of a specimen group (Loy *et al.* 1999). Bookstein (1982) described morphometrics as "the biometric study of effects upon form", "form" being the intrinsic combination of size and shape. Form was determined by assigning homologous landmarks that exploited the data of curvatures, corners, or surfaces that may serve as points of net biological change or variation (Rohlf *et al.* 1985; Rohlf 2000). As biological inquiry became more quantitative, modern statistical methods within the discipline of morphometrics were employed to provide a new compilation of tools used for discrimination processes (Richtsmeier *et al.* 2002; Walker 2000). The geometry of biological form in two- or three-dimensional space and the efforts to preserve the physical integrity of form

developed into the most recent form of geometric morphometrics, a fusion of geometry and biology (Bookstein 1982, 1990; Ferson *et al.* 1985).

Because craniometry, anatomy and palaeontology had already distinguished classic anatomical definitions of biological landmarks, these could now be used to accurately obtain coordinate locations and provide researchers with homologous data points on which to base their morphometric analyses. Cranial morphology and the quantification of shape characteristics through geometric morphometrics have been studied at length by biologists to typify the varying orders of mammals and to assign crania to possible groups for more discrimination in species determination (e.g., Adams 1999; Pretorius and Scholtz 2001; Ross *et al.* 1999). Morphometric analysis followed logically by using these established landmarks in anthropological studies as well. Only in the second half of this morphometric era has anthropology gained with quantification techniques applied to the shapes and contours of the human skeleton. While anthropology has gained information in the morphometric analysis of two-dimensional and three-dimensional skeletal features, challenges in landmark assignments have also been recognized as a potential limiting factor with geometric morphometrics (von Cramon-Taubadel *et al.* 2007).

Geometric morphometrics, then, is the analysis of a set of digitized landmark coordinates, with each set recording the form of the specimen (form = shape + size). Landmarks are specific locations on biological forms and are recorded as two- or three-dimensional coordinates. These coordinates, when visualized and recorded on a collection of objects of the same biological form, are then known to be corresponding, or homologous (Richtsmeier 2002). Homologous landmarks remove the effects of variation in orientation and dimension of specimens, with the remaining distinctions representing shape variation. This approach detects shape differences with more statistical power as landmark coordinates can obtain more data regarding shape, resulting in different and perhaps enhanced visualization of the results than conventional methods (Rohlf 2003).

Morphometric methods are simply tools to help define the difference between forms via geometry. Two methods most commonly used (and those utilized in this study) are deformation methods and linear distance-based methods.

- Deformation Methods:

  Deformation methods take the area or volume of a reference form (normally a precisely symmetrical grid structure) and deform it to correspond with that of the target form. Sir D'Arcy Thompson's work (Thompson 1992) is the first and best-known instance of the use of deformation techniques for the demonstration of the difference between forms. He created "transformation grids" where a two-dimensional grid was placed over one structure (or form), and the grid was transformed to correspond to the morphology of the second structure (or form). The "transformation" in the grid described the difference in structures. Thompson's work imparted information more about outlines than to landmarks, and he did not propose any quantitative method for creating these grids.

Thin-plate splines are the modern configuration of Thompson's "transformation grid" efforts. Thin-plate splines use chosen functions to chart the relative location of points in an initial configuration to their precise locations in a corresponding target form precisely. These functions also can predict how points that lie in those areas between landmarks in an initial form are arranged on the target form. Richtsmeier *et al.* (2002) described the process as "...placing a continuous and bendable surface (or plate) over the area or volume encompassed by the landmarks. This plate is then deformed in such a way that: 1) corresponding landmarks in the two objects are mapped to one another exactly; and 2) the quantity of a specific parameter, often bending energy, within the function is minimized. This

means that only the minimal amount of energy required to bend the plate to conform to the target object is used" (pg. 79).

- Linear distance-based methods:

  These methods evaluate the linear distances that connect landmark pairs in one structure to analogous linear distances in another structure. They also provide data regarding the differences in length and magnitude of linear variations of these distances. This not only shows the amount of distance between corresponding forms, but also shows where the differences occur and in what direction they are exhibiting their modifications. These variations are considered "vector" variations.

Robust statistical tests built into analytical software have benefited from additional computer models, which allow researchers to easily visualize results in morphometric studies. James F. Rohlf developed the 'tps' series of programs that calculate statistics and provide easily created thin-plate spline grids to visualize the quantifiable changes in form (Rohlf 2000). The 'tps' series consists of a collection of programs utilized in many of the past studies performed on morphological analysis of form, and were employed in this study as well.

Geometric morphometrics can provide indications of explicit variation locations on a specific skeletal element. This means that the divergence between males and females in a specific location on a skeletal element can be shown to exist, and the direction of that variation may be observed. In addition, classification results and accuracy are comparable to traditional discriminant analysis. For example, Hennessy and Stringer (2002) provided a summary of craniofacial variation that allocated modern humans to regional geographic groups based on three-dimensional landmark analysis using classic anatomical markers already established as possible points of craniofacial diversity.

Applications of morphometrics on hard tissue to determine variances between the sexes have included both cranial and post-cranial elements (Marcus *et al.* 2000). The efficacy of morphometric analysis to determine sexual dimorphism in the skeleton has been established and utilized in numerous studies to observe the quantifiable variances between the male and female shape (e.g., Franklin *et al.* 2006; Pretorius and Steyn 2005; Pretorius *et al.* 2006). These applications have led to the possibility that size and shape are never biologically independent, but the quantification of shape and the "normalization" of size differences will assist in an attempt to reduce the influence of size on the shape of an element being studied.

Comparing the relative locations of features and how they differ in arrangement from the "mean" form of a skeletal element has been established as the greatest asset in using geometric morphometrics to determine the level of sexual dimorphism in skeletal features. Results that may be expected from geometric morphometrics on the pelvic region may include variation in the shape and contours of the subpubic concavity; the distinct robusticity or gracile nature of the ischio-pubic index; the elongation and rectangular shape of the subpubic angle in females as opposed to the relatively blunt and triangular shape of the male subpubic angle; and the width of the greater sciatic notch. Results expected from analysis of the distal and posterior humerus may include differences in olecranon fossa shape; the extension of the trochlea past the distal margin of the capitulum; and the angling or parallel nature of the medial epicondyle as it projects from the trochlear profile.

Sexual dimorphism in humans has long been the topic of research, study, and technical interpretation. Changes in bone with the onset of age (both macroscopically and microscopically) have also been subjected to consistent scrutiny. The history of research done on these topics forms the foundation of observing traits and measurements in the human postcranial skeleton that may or may not change when age increases.

CHAPTER 3

MATERIALS AND METHODS

3.1

Sample

The skeletal sample in this study originated from the Pretoria Bone Collection at the Department of Anatomy, University of Pretoria and the Raymond Dart Collection at the University of Witwatersrand. The Pretoria Bone Collection was established in partnership with the Department of Anatomy and the Medical School at the University of Pretoria, South Africa in 1987. These individuals, being both donated and unclaimed by relatives, are received as cadaver teaching specimens first, then macerated and stored in acid-free boxes for research purposes (L'Abbe *et al.*, 2005). The collection houses several biologically distinct groups of individuals, the most common being black South African males. Also represented are black South African females and white South African males and females. Bodies are acquired by either direct donation or as an unclaimed specimen.

Those wishing to donate their body may complete paperwork before death occurs; in addition, an individual's next of kin may donate a body for research and study after death has occurred. Unclaimed bodies are handled differently in the fact that they are transported directly from the hospital where the individual died to the University for study and research, without the traditional consent form required according to the Human Tissues Act (1983). In addition, age restrictions exist with tissue donation; so all individuals over the age of 65 or those who have died from specific pathological conditions are not appropriate for tissue donation. These specimens again are transported immediately to the University of Pretoria Medical School campus for embalming and subsequent teaching purposes.

Ages within the sample range from 19 to 94 years. The postcranial long bones of 404 adult males and 189 adult females were used in this study (Table 3.1). The difference between numbers of males and females reflects their disproportionate representation in the collection. The sample size varied among the various measurements, due to the fact that some skeletal elements had broken shafts or absent epiphyseal ends. These samples were not wholly excluded because of the goal sample size of 500.

The sample was divided into categories of "young" (50 years of age or younger) and "old" (over 50 years of age). Because of the abundance of specimens over the age of 50, all individuals in the young age group that were deemed appropriate for analysis were utilized in this study. The age boundary between young and old was developed based on the amount of data from scientific sources (osteoporosis journals, geriatric publications) that described bone modification occurring not only in the second and third decades of life, but well within the seventh and eighth decades. Ultimately, individuals (women) over 50 were clearly postmenopausal, and thus the discriminating boundary was 50 years of age. Skeletal elements that exhibited acute pathology or healed trauma at the measurement site were excluded. Bones with age-related pathology were not excluded due to the information they provide regarding age-related changes. Clearly defined osteophytes were not included in the measurements. The Pretoria Bone Collection was primarily used for compiling data, however where specimens in a specific group were lacking, the nearby Raymond Dart Skeletal Collection was utilized as well. The Dart Collection offered a small percentage of specimens, but was helpful in supplementing information on young white females, a population that is in short supply in the Pretoria Bone Collection.

3.2

Data Collection

A data sheet was created to record measurements and appropriate information (Appendix A). From this information, a spreadsheet was generated with appropriate box and cadaver numbers as well as the approximate sample size for each population. The spreadsheet did not list the known age or sex of the specimens, so as not to introduce bias in the assessment of characteristics. The goal was not to illuminate the differences between South African blacks and South African whites, but to determine whether men and women change morphologically with age, and to what extent. Non-metric visual traits were recorded on the data sheet first. Quantitative data was collected second so as not to bias the observer with potential morphological size information that indicated the sex of the individual.

3.2.1

Data collection of non-metric information

Collection of data from the postcranial skeleton was taken from one long bone (the humerus) and one irregular bone (the pelvis) in order to determine sex by visual methods. Non-metric morphology of long bones has not been conventionally employed to determine the sex of skeletal specimens. However, Rogers (1999) defined several traits of the distal humerus that proved sexually dimorphic on a statistically significant level. These traits were subsequently used to determine skeletal sex with numerous populations, producing accurate results as well (Wanek 2002). These results reinforced the assertion that traits from the distal humeral articular surface were, in fact, sexually dimorphic. Therefore, the humerus (the distal and posterior aspect of the humerus, specifically) was identified as one of the two skeletal elements to be used in this study to record non-metric information on sex.

Traditional visual characteristics used to determine sex from the postcranial skeleton, on most occasions, utilize the pelvis. Pelvic morphology has been

confirmed on numerous occasions as being highly sexually dimorphic and quite accurate in the determination of skeletal sex. The os coxae, therefore, was used in this study to apply classic non-metric attributes to all specimens.

Attributes from both skeletal elements and the ultimate estimated sex were recorded separately, first from the humerus and next from the pelvis. This order of documentation was used in an effort to not bias the observer with classic pelvic morphology when looking at the lesser-known traits of the humerus.

3.2.2

Data collection of non-metric information from the humerus

Four visual indicators of sex in the distal and posterior humerus were defined as "medial epicondylar symmetry", "trochlear extension", "olecranon fossa shape", and "angle of the medial epicondyle". Rogers (1999) first described these characteristics. Modification of these characteristics were subsequently made by Wanek (2002) and utilized successfully. Descriptions of the typical male and female morphology of the distal humerus are described in Table 3.2. In addition, visual representations of each characteristic are shown in Figures 3.1 to 3.8. Data on the left humeri were used for analysis.

Non-metric traits were first observed and recorded on the data sheet. A degree of "femaleness" and "maleness" of the trait was determined by assigning the most obvious male features a [1], an intermediate yet still discernable male feature a [2], an ambiguous feature a [3], an intermediate yet still obviously female feature a [4], and a clearly female feature a [5]. The combined total of the numerical values of traits were used to make an estimation of sex for the humerus as a whole. A particular humerus could therefore obtain a maximum score of 20, if it was hyperfeminine. A total score of four through 11 indicated that the specimen was a male; a score of 12 indicated an ambiguous specimen; and a total score of 13 through 20 indicated a female specimen. Finally, either a [1]/ male or [5]/ female was

recorded on the data sheet and for data input into subsequent spreadsheets for statistical analysis. "Five" was given to females under the categories of "known sex" and "estimated sex" because it best described females to those interpreting the data. The number five always illustrated an unambiguous female when used with all single variable determinations; it was logical to extend this representation of females in the "known" and "estimated" fields of the database. Just as a "five" value showed an obvious female, a "one" represents the most blatant and robust of male traits. A "one", then, was used to denote males in the same categories of "known sex" and "estimated sex" within the spreadsheet whenever applicable.

This scoring method is illustrated by the following two examples:

- Reference Number: 5569
  Box Number: 1140
  Medial epicondylar symmetry: 5
  Trochlear extension: 2
  Olecranon fossa shape: 3
  Angle of the medial epicondyle: 1
  - Final score = 11
    Final determination = [1]/ Male

(This specimen was eventually revealed as a black male, 23 years old.)

- Reference Number: 2228
  Box Number: 3069
  Medial epicondylar symmetry: 4
  Trochlear extension: 4
  Olecranon fossa shape: 5
  Medial epicondylar angle: 1
  - Final score = 14
    Final determination = [5]/ Female

(This specimen was eventually revealed as a white female, 43 years old.)

3.2.3

Data collection of non-metric information from the pelvis

Four well-defined and proven characteristics of pelvic morphology were used for the determination of sex. These traits included the length of the subpubic concavity, the width of the subpubic angle, the ischio-pubic ramus width and the width of the greater sciatic notch (Bass 1995; Steele and Bramblett 1988).

Descriptions of the typical male and female characteristics of the pelvis are given in Table 3.3.

These suites of characteristics have been tested consistently throughout the last four decades of physical anthropological research, and proved to be accurate in assisting in the determination of sex from the os coxae (Bass 1995). Visual representations of each pelvic characteristic are shown in Figures 3.9 to 3.16. Data on the left os coxa was used for analysis.

Observations of the os coxae were collected after all humerus data was recorded for each specimen. This sequence of events was established for the same reason as quantitative data was collected last, so as not to bias the observer with well-known and well-defined criteria for male and female pelvic morphology. A gradient value of 1-5 was recorded next to each of the characteristics of the os coxae of each individual. These values paralleled the grades assigned to non-metric traits of the humerus.

3.2.4

Data collection of metric information from long bones

Measurements from all six major long bones were included in this study. In all of these skeletal elements, the maximum diameters of proximal and distal articular ends, maximum midshaft diameters, and circumferences (when applicable) were collected. Twenty-three total measurements from long bones were gathered. All measurements and descriptions were based on established data collection protocols in order to be as comprehensible and unambiguous as possible (Moore-Jansen *et al.*, 1994; Bass 1995). Measurements and their descriptions of the postcranial skeleton appear in Table 3.4.

Locations of each long bone measurement were chosen based on numerous criteria. All major postcranial long bones were included to provide a comprehensive observation with regard to where metric changes were taking place, if any were

detected. The articular ends (proximal and distal) were both measured based on their importance as joint surfaces and recipients of stress throughout the various decades of life. It was determined that if changes with age were occurring, these changes may be observable in these articular joint surfaces. Maximum midshaft diameters of all long bones were collected based on past research indicating that cortical thickness changes with age, medullary cavities expand with age, and the combination of these traits possibly contributing to an increase in the diameter of long bones (Epker *et al.*; Jowsey 1960; Thompson 1980). Midshaft circumferences of tubular long bones (humerus and femur) were collected for the same reason. It is also these measurements (articular ends and midshaft circumferences) that have been shown to be most dimorphic when using metrics – e.g., in those discriminant function formulae. These locations are the sites that are most sexually dimorphic and may change with age, thus influencing the accuracy of developed formulae.

Overall, the reasoning behind the choice of long bone measurement sites was largely due to logical deductions in regard to where skeletal changes may be taking place. Past research indicated that joint surfaces might be adversely affected (with a result of net bone gain or loss) in the advancement of age in humans. The details of each long bone measurement are shown in Figures 3.17 - 3.24. Data on left bones were used for analysis.

3.3

Statistical analysis of metric and non-metric data

Statistics are defined as "a quantitative characteristic of a sample" (Slitor, 1987). Statistical analyses are ways of discriminating between and within groups or samples. If an individual is to be classified into a defined group based on certain measurements, they must be compared to a known sample and placed with a certain amount of accuracy into the most-correct group based on these variables. Basic

descriptive statistics, including means, standard deviations, and ranges were done for all metric data. Definitions of each are as follows:

Mean: the average of the data set. The mean is equal to the sum of the measurements divided by the number of measurements.

Standard deviation: a measure of variability or variation when considering all data. The standard deviation is calculated by finding the mean, calculating the deviation from the mean for each observation, squaring these deviations, averaging the squared deviations, and taking the square root of this average (Slitor, 1987). This is essentially equal to the positive square root of the variance. It is a measure of the dispersion of the frequency distribution, or a statistical measure of the spread or variability between a group of measurements.

Range: the difference between the highest and the lowest values in the data set of measurements. The range provides the extreme variation in the sample.

An analysis of variance (ANOVA) was also computed for all metric data to observe irregularity between elements of the sample. Analysis of variance is a procedure that computes the amount of variability attributed to each one of a variety of components. Specifically, it compares the means of two or more groups of subjects that vary on a single independent variable (Cronk 1999). ANOVA can also be described as the measurement of distance between individual distributions.

In this case, groups with categorized metric means were defined as "male" and "female", while the single independent variable in which they vary was the measurement provided. A one-way ANOVA comparing male metric data and female metric data was computed. A significance value (F-ratio) was provided by this analysis, and from this value an assessment of the variability between two groups (e.g., male and female) was determined. Theoretically, as the F-ratio goes up, the p-value goes down (i.e., more confidence there is a difference between the male and female means). If the F-ratio is large (much greater than 1), it suggests that a possible group effect exists.

The p-value is a probability with a value ranging from zero to one. A p-value is a measure of how much evidence there is against the null hypothesis. The smaller the p-value, the more evidence against the null hypothesis (and the larger the F-ratio). The general rule is that a small p-value is evidence against the null hypothesis, while a large p-value means little or no evidence against the null hypothesis (Kendall and Stuart 1979). Traditionally, researchers will reject the null hypothesis if the p-value is less than 0.05.

The comparison of groups followed a progression of analysis set forth to observe all possible variations in skeletal change between assemblages. All females and all males in the study sample were first compared to establish that a size component existed between the two. This is a common observation seen in all populations, in which males are metrically larger than their female counterparts.

Second, males and females were separated into population categories and compared, e.g., white males were compared to white females; black males were compared to black females. This comparison was performed to confirm that this sexually dimorphic size difference not only occurred when the populations were pooled, but when the populations were separated as well. Information on the relative size of each population was also obtained from this comparison.

Third, females were separated into the two groups ("black females" and "white females"), and their measurements were compared. This comparison was performed in an effort to possibly pool the two groups if they resembled each other metrically.

The metric means of young females (50 years of age and under) were compared to the metric means of old females (over 50 years of age) for each skeletal measurement site, and for both groups. If a statistically significant increase or decrease was observed with the onset of age at a particular skeletal measurement site, this site was compared to the equivalent metric mean for the corresponding male population. For example, if the diameter of the head of the humerus increased

significantly with the onset of age in white females, then the humeral head diameter mean for old white females would be compared to the mean humeral head diameter of old white males to determine if any metric overlap of data existed at this skeletal site.

This progression of analysis repeated itself with the male sample. Males were separated, and the metric means of young males (50 years of age and under) were compared to the metric means of old males (over 50 years of age) for each skeletal measurement site. If a statistically significant change with age occurred (either a decrease or an increase in metric size) this metric mean was compared to the corresponding female metric mean to determine if overlap existed between the sexes. These observations provided information on the increase or decrease of robusticity in the skeletal measurement location, which could be extrapolated as an increase or decrease in sexual dimorphism.

To test for intra-observer repeatability in the metric analysis, 15 male specimens and 15 female specimens were randomly selected and re-measured after all initial data was collected. The repeated metric data was statistically compared to the original data set using a one-way analysis of variance (ANOVA).

To test for inter-observer repeatability, 30 specimens were once again selected and an independent observer re-measured several long bone sites (four from the humerus) and all four pelvic measurements. The independent observer was someone not involved in the study, but who had limited experience with metric analysis. Measurement techniques were described and reviewed with the observer. This metric data collected by the observer was statistically compared to the original dataset using a one-way ANOVA.

Pearson's chi square test was performed initially on all nonparametric data of the humerus and os coxae to establish association and significance between variables. A chi square test uses nominal scale data to compare samples to theoretical distributions, and assess relationships between nominal variables. It can

also be described as a measure of agreement between the observed and expected values (Butler 2000). This statistic is more likely to establish evidence that (1) the relationship is strong (or weak), (2) the sample size is large, and/or (3) the number of values of the two associated variables is large. Statisticians commonly interpret a chi square probability of 0.05 or less as justification for rejecting the null hypothesis. This implies that the one variable is unrelated (that is, only randomly related) to another variable.

After significance between groups (males vs. females, black males vs. black females, white males vs. white females) was determined, a comparison of young and old individuals in a specific sex-population affiliation was performed to determine if a significant decline in the classification accuracy was present, i.e., if the accuracy in predicting sex from a certain skeletal feature decreased with the onset of advanced age.

3.4

Data collection for geometric morphometric analysis

The sample size used for geometric morphometric analysis was set at 50 individuals of each age, ancestry, and sex group. The ideal total sample size was 400 specimens (50 per age/ ancestry group) for a geometric morphometric examination of four sexually dimorphic features. The Pretoria Bone Collection and the Raymond Dart Skeletal collection combined provided an amalgamation of young and old individuals. The reality of both skeletal collections, however, is that they house a disproportionate amount of older individuals, whose population falls within the "black" category. The geometric morphometric analyses were performed regardless of this fact and based on the assumption that any amount of data on young individuals would make the study valuable.

When all data was collected and all digital images captured, young white females were the least represented (n=13) followed by young white males (n=24). Young black males (n=57) and young black females (n=50) supplemented the data sufficiently to provide insight regarding common morphology in young individuals.

Standardized landmarks were chosen for four two-dimensional views for geometric morphometric analyses. Two views of the humerus were used; a two-dimensional perspective of the distal and inferior humerus which documented the angle of the medial epicondyle (referred to as "EPI") and a two-dimensional perspective of the distal and posterior humerus which documented the olecranon fossa shape and trochlear extension (referred to as "OL"). Two views of the os coxae were used; a two-dimensional representation of the subpubic angle and subpubic concavity (referred to as "SUB") and a two-dimensional perspective of the greater sciatic notch (referred to as "SCI"). Each of the four perspectives was utilized in order to quantify shape and form differences observed in these features. Definitions of each feature are listed below:

- **EPI:** this view captured the distinct feature of the medial epicondylar angle from the inferior aspect of the humerus.

- **OL**: this view captured features specifically of the distal and posterior humeral aspect. It included the olecranon fossa shape and trochlear extension, thus corresponding to two non-metric visual traits.

- **SUB**: this view captured pelvic features such as the subpubic concavity and the subpubic angle, two characteristics that directly corresponded to non-metric visual traits were observed. It also provided information on the shape of the obturator foramen. Obturator foramen landmarks were chosen

because this skeletal feature's centralized location within the two-dimensional perspective, and its relationship to other landmarks that were difficult to assign without using corresponding points from the foramen.

- **SCI:** this view captured the anatomy and morphology of the greater sciatic notch.

Because each of the four views was considerably different from each other, standardization of bone positioning and landmarks will be described separately. Figures 3.25 - 3.28 depict the anatomical locations of homologous landmarks chosen for geometric morphometric analysis.

As documented in Appendix B-I (the specimens utilized for each sex and ancestry group) the number of actual digital photographs for each view varied for several reasons. The original goal of the study was to create digital images of 50 specimens per group, resulting in 400 photographs total. All specimens were chosen randomly, and not based on past knowledge of the skeletal sample. Because of this random selection of specimens from the collection, numerous individuals in the study exhibited damage, degradation, or the absence of specific element features required to capture a digital image. Thus, one specimen may have both images of the distal humerus present, but only one image of the os coxa present due to the degradation of the pubis or the absence of the ischium. Osseous elements used for geometric morphometrics must be placed in a standardized position for each digital image taken. In order to achieve a controlled position for the bone, the same specific procedure was used, depending on which perspective was being photographed.

3.4.1

Image capture of the EPI view of the humerus

The left humerus was placed on grid paper on an osteometric board with the posterior side facing upwards. The superior surface of the humeral head and greater tubercle touched the upper left-hand-corners of the osteometric board. The distal end of the humerus was then aligned along a grid paper axis to place the trochlear constriction (the indentation made between the capitulum and the trochlea) in a standardized location, 11 centimetres to the right of the left margin of the osteometric board. This was to eliminate the variation of curvature that exists in this element (which was not an important characteristic to capture). The camera lens was at a perpendicular angle to the bone surface.

Photographs were taken of the inferior "spool" feature of the distal humerus with a Cannon SureShot 95 digital camera. The camera was placed in a fixed position in front of the inferior feature, 60 centimetres from the top margin of the osteometric board. A reference number corresponding to the specimen number was placed in the image for consistency in image file maintenance. The viewfinder was focused on the middle of the bone and the image filled the frame at all times. The captured images were saved and recorded with reference numbers onto a computer, and 19 homologous landmarks were assigned to features for geometric morphometric analysis.

Landmarks were chosen to mirror the morphology observed in the visual techniques used for the non-metric portion of this study. Nineteen distinct points along the surface of the inferior humerus were chosen to best characterize the form of this skeletal element. The captured images were entered into a computer and the 19 landmarks were assigned to each humerus to use for geometric morphometric analysis. The program tpsDig allowed for the assignment of each homologous landmark chosen. The landmarks assigned were as follows (see Figure 3.25):

- Landmark 1 was the medial margin of the lateral epicondyle, on top of the ridge of bone that constitutes the posterior surface of the capitulum.

- Landmark 2 was situated halfway between Landmark 1 and Landmark 3
- Landmark 3 was the lowest portion of the posterior spool, which constituted the inferior margin of the olecranon fossa.
- Landmark 4 was halfway between Landmark 3 and Landmark 5.
- Landmark 5 was the most superior point of the medial margin/ ridge of the posterior trochlea.
- Landmark 6 was the superior "root" of the medial epicondyle; where the posterior edge of the medial epicondyle meets the vertical ridge of the trochlea.
- Landmark 7 was halfway between Landmark 6 and Landmark 8.
- Landmark 8 was halfway between Landmark 7 and Landmark 9.
- Landmark 9 was halfway between Landmark 8 and Landmark 10.
- Landmark 10 was the most medial point on the medial epicondyle.
- Landmark 11 was halfway between Landmark 10 and Landmark 12.
- Landmark 12 was halfway between Landmark 11 and Landmark 13.
- Landmark 13 was halfway between Landmark 12 and Landmark 14.
- Landmark 14 was the inferior "root" of the medial epicondyle; where the inferior edge of the medial epicondyle meets the vertical ridge of the trochlea.
- Landmark 15 was the inferior edge of trochlea. This landmark was placed where the straight vertical edge of the trochlea becomes curved again.
- Landmark16 was the most constricted point on the anterior trochlear "spool".
- Landmark 17 was the most constricted point on the anterior capitulum "spool".
- Landmark 18 was the inferior border of the capitulum. This landmark was placed on the point where the curved edge becomes a distinct ridge.
- Landmark 19 was the lateral-most point of the lateral epicondyle.

Landmarks 7 through 19 and 11 through 13 were based around Landmarks 6, 10, and 14 (the fixed, unambiguous locations on the medial epicondyle). Landmarks

7 through 9 and 11 through 13 should be an approximately equal distance from one to another. These landmarks cannot be exactly equidistant, as it is not possible to assign equidistant landmarks on a curved surface with no border except "superior" root and "inferior" root. These landmarks were assigned based on the supposition that a landmark placed consistently along the surface of the medial epicondyle would correctly record its general form and angle.

3.4.2

Image capture of the OL view of the humerus

The humerus was placed on graph paper on an osteometric board with the posterior side facing upwards. The superior surface of the humeral head and greater tubercle touched the upper left-hand-corners of the osteometric board, as in the previous perspective, "EPI". The distal end of the humerus was then aligned along a grid paper axis to place the trochlear constriction in a standardized location, 11 centimetres to the right of the left margin of the osteometric board. This ensured that the inferior edges of the trochlea and capitulum were correctly aligned with each other.

Images were captured with the Canon SureShot 95 digital camera mounted on a small tripod 30 centimetres above the surface of the bone. A reference number corresponding to the specimen number was placed in the image for consistency in image file maintenance. The image filled the frame each time an image was captured. The captured images were entered into a computer and the 15 landmarks were assigned to each humerus to use for geometric morphometric analysis. The program tpsDig allowed for the assignment of each homologous landmark chosen. These distinct points along the surface of the distal and posterior humerus were chosen to best characterize the form of this skeletal element. The landmarks assigned were as follows (see Figure 3.26):

- Landmark 1 was placed on the supra-condylar ridge, aligned with the superior margin of the olecranon fossa. The grid paper placed underneath the bone was used to assist in assigning this landmark, based on a grid line's linear progression across the bone, which most accurately showed the positioning of the upper margin of the olecranon fossa.
- Landmark 2 was the medial ridge of the humerus, placed on the supra-condylar ridge, aligned with the superior margin of the olecranon fossa.
- Landmark 3 was the most lateral point of olecranon fossa seen on the posterior surface. This landmark was not placed within the fossa itself, but on the lateral edge of the fossa.
- Landmark 4 was the most medial point of the olecranon fossa, also placed on the surface of the bone as opposed to within the fossa itself.
- Landmark 5 was the most superior point of the olecranon fossa.
- Landmark 6 was the inferior edge of olecranon fossa, directly in the middle. This landmark was placed halfway between landmark 3 and 4, and was placed on the smooth bone "ridge" that begins there.
- Landmark 7 was halfway between Landmark 3 and Landmark 5.
- Landmark 8 was halfway between Landmark 4 and Landmark 5.
- Landmark 9 was halfway between Landmark 3 and Landmark 6, on the smooth bone "ridge" that begins in this location.
- Landmark 10 was halfway between Landmark 4 and Landmark 6, where the smooth edge of bone begins in this location.
- Landmark 11 was the most lateral edge of the lateral epicondyle.
- Landmark 12 was the most medial point on the medial epicondyle.
- Landmark 13 was the inferior edge of capitulum, at the point of the where the curved edge becomes a distinct ridge.
- Landmark 14 was the most constricted point of the posterior trochlear "spool".

- Landmark 15 was the inferior edge of trochlea, at the junction where the straight ridge became curved.

3.4.3

Image capture for the SUB view of the os coxa

An osteometric board with grid paper along both the flat surface and along the short vertical surface was used to place the left os coxa into position to capture the form of the subpubic angle and subpubic concavity. The superior margin of the iliac crest was placed against the long vertical edge of the osteometric board, while the edge of the acetabulum that aligns with the pubis was placed against the short vertical edge of the osteometric board. This, in turn, placed the entire pubic region against the short vertical edge. The bone rested on the posterior inferior iliac spine and the medial surface of the ischium, as well as the posterior edge of the acetabulum.

Images were captured with the Canon SureShot 95 digital camera. The camera was placed in a fixed position in front of the pelvis, 60 centimetres from the top margin of the osteometric board. The right edge of the camera was placed 19 centimetres to the left of the long right vertical edge of the osteometric board to standardize the position of the image. A reference number corresponding to the specimen number was placed in the image for consistency in image file maintenance. The image filled the frame each time.

Twenty-eight distinct points along the surface of the pubis, ischium, and obturator foramen were chosen to best characterize the form of this skeletal element. Landmarks 1 through 13 are along the interior border of the obturator foramen. The landmarks assigned were as follows (see Figure 3.27):

- Landmark 1 was the junction where the body of the pubis meets the obturator groove. This point is indicated by a visible “overlap” of bone.

- Landmark 2 was the lowest point of the obturator foramen. A linear junction on the grid paper assisted in the assignment of this landmark.
- Landmark 3 was the highest point, or "apex" of the obturator foramen.
- Landmark 4 was the narrowest point on the superior ventral margin of the obturator foramen.
- Landmark 5 was halfway between Landmark 2 and Landmark 4.
- Landmark 6 was halfway between Landmark 1 and Landmark 2.
- Landmark 7 was halfway between Landmark 1 and Landmark 3.
- Landmark 8 was halfway between Landmark 3 and Landmark 4.
- Landmark 9 was halfway between Landmark 4 and Landmark 5.
- Landmarks 10 and 11 were two points spaced evenly between Landmarks 2 and 5, Landmark 10 placed superiorly, Landmark 11 placed inferiorly.
- Landmark 12 was halfway between Landmark 2 and Landmark 6.
- Landmark 13 was halfway between Landmark 1 and Landmark 6.
- Landmark 14 was the superior edge of the pubis, positioned at a 45-degree angle from Landmark 1.
- Landmark 15 was the superior edge of pubic symphysis.
- Landmark 16 was halfway between Landmark 14 and Landmark 15.
- Landmark 17 was halfway between Landmark 14 and Landmark 16.
- Landmark 18 was halfway between Landmark 15 and Landmark 16.
- Landmark 19 was the most inferior edge of pubis. This location may or may not be the edge of pubic symphysis.
- Landmark 20 was halfway between Landmark 15 and Landmark 19.
- Landmark 21 was the shortest distance from landmark 4 on the ischial surface. This could also be considered the thinnest portion of the ischium.
- Landmark 22 was a point directly across from landmark 2 on a horizontal plane. The placement of the vertical grid paper was used for guidance in assigning this point.

- Landmark 23 was halfway between Landmark 19 and Landmark 21.
- Landmark 24 was halfway between Landmark 21 and Landmark 22.
- Landmark 25 was halfway between Landmark 19 and Landmark 23.
- Landmark 26 was halfway between Landmark 21 and Landmark 23.
- Landmark 27 was halfway between Landmark 21 and Landmark 24.
- Landmark 28 was halfway between Landmark 22 and Landmark 24.

Eighteen of the 28 landmarks assigned to this view were based on placing these locations between each other or between two fixed landmarks used as foundational points of morphology. These landmarks cannot be exactly equidistant, as it is not possible to assign equidistant landmarks on a curved surface with no border except "most superior edge" and "most inferior edge". These landmarks were assigned based on the theory that a landmark placed consistently along the surface of the ischium would correctly record its general form and curvature.

3.4.4

Image capture of the SCI view of the os coxa

The position of the left pelvic bone did not change from the "SUB" view to the "SCI" view; only the position and angle of camera were altered to capture the features of the greater sciatic notch. Thus, the superior margin of the iliac crest was again placed against the long vertical edge of the osteometric board, while the edge of the acetabulum that aligns with the pubis was placed against the short vertical edge of the osteometric board. The bone rested on the posterior inferior iliac spine and the medial surface of the ischium, as well as the posterior edge of the acetabulum.

Images were captured with the Canon SureShot 95 digital camera, which was mounted on a small tripod 40 centimetres above the bone's surface. A reference number corresponding to the specimen number was placed in the image for

consistency in image file maintenance. The image of the greater sciatic notch filled the frame each time an image was captured.

Landmarks were chosen based on past geometric morphometric studies (Steyn *et al.* 2004), and mirrored the morphology observed in the visual techniques used for the non-metric portion of this study. The landmarks assigned were as follows (see Figure 3.28):

- Landmark 1 was the most projecting point of the spina ischiadica, or inferior ischial spine.
- Landmark 2 was the point of maximum curvature of the greater sciatic notch.
- Landmark 3 was the end of the sciatic notch before the bone curves backwards towards the auricular surface.
- Landmark 4 was halfway between Landmark 2 and Landmark 3.

Landmark 5 was halfway between Landmark 1 and Landmark 2.

3.5

Statistical analysis of geometric morphometric data

The entire dataset for each view (EPI, OL, SUB and SCI) was divided first into subgroups of two, namely males (M) and females (F) to initially provide evidence of morphological differences between the sexes. Second, the dataset was separated into four different subgroups; young females (YF), old females (OF), young males (YM), and old males (OM). This was to illuminate differences with the onset of age between members of the same sex group, i.e., young females and old females. Finally, a third set of eight subgroups was created to visualize potential changes with the onset of age between populations. These subgroups were categorized as young black females (YBF), old black females (OBF), young white females (YWF), old white females (OWF), young black males (YBM), old black males (OBM), young white males (YWM), and old white males (OWM).

The homologous landmarks for each perspective were assigned on the digitized images of the distal humerus and os coxae using the program tpsDig (defined below). Generalized least-squares Procrustes analysis was used to compute the average shape for each sample (Hennessy and Stringer 2002; Rohlf 2000; Loy *et al.* 1999). Landmarks were then used to perform geometric morphometric analyses on each of the four perspectives in a series of steps, based on the tps program **tpsDig**, (FJ Rohlf, Version 1.31), **tpsSplin** (FJ Rohlf, Version 1.14), **tpsRelw** (FJ Rohlf, Version 1.25), **CoorGen**, **CVAGen6- IMP**, and **TwoGroup6-IMP** (Sheets 2001).

- **tpsDig:**

The standardized landmarks (described above) were digitized using tpsDig. The tpsDig-program makes collection and maintenance of landmark data from digitized images simpler. The program also creates statistical results from landmark data. It is used to indicate the position of landmarks in an initial file and creates specific, discrete file names containing the images of specimens. The data is saved as tps data-files and these files are then used with the other tps-programs (e.g., tpsSplin and tpsRelw) (Slice *et al.* 2005).

In order to study the shape differences between groups, the average, or consensus configuration of landmarks for each of these two groups (males and females) was computed using tpsSplin. From this it was possible to visually assess whether any differences existed between the males and females for each view.

- **tpsSplin:**

The tpsSplin-program is used to compare the same homologous landmarks in different specimens by utilizing thin-plate spline transformations. Principal and partial warps were also created and used. A preliminary reference shape is produced; this is the average shape of the entire sample population, and is

designated by a precise perpendicular grid pattern exhibiting no deformations of 90-degree angles with the homologous landmarks included. The thin-plate splines for each specimen illustrate the deformation (or incongruence) of this grid. Deformation grids of the consensus configurations of the groups made it possible to determine where the variation was for each perspective. The consensus thin-plate splines were also viewed in "vector mode" to determine which landmarks were responsible for the greatest amount of variation. In other words, vector thin-plate splines indicate where and by how much the landmarks of two specimens in the sample group differ from each other (Scholtz 2006).

- **tpsRelw:**

Differences in shape were determined and analyzed using tpsRelw. This program facilitates the statistical analysis of geometric morphometric landmark data by showing the distribution of specimens within the groups that are to be compared to each other (e.g., young males and old males) in order to scrutinize intra-sample distinctions. This is presented in graph form to make the representation of any variation between groups in a sample population possible to visualize.

The Relative Warp Analysis (RWA) was performed in order to determine general trends in shape between the two sexes and with the onset of age. From this analysis it was possible to see whether a definite separation between the male and female dataset existed or whether there was no clear distinction between the shape of the two sexes.

- **CoordGen:**

The CoordGen-program was used to translate tps data-files to "Bookstein's Coordinates" (or BC) format which is subsequently used with other programs in the IMP package (e.g. CVAGen6 and TwoGroup). Bookstein's Coordinates are described as an arrangement of shape coordinates consisting of a compilation of

landmarks "1, 2...15" whose structures have been rescaled to a standardized scale. Thus, landmarks 1 and 2 are fixed at (0, 0) and (1, 0) respectively, in a Cartesian coordinate system (Sheets 2001). This is used for two-dimensional data.

- **CVAGen6:**

Statistically significant differences were determined between each group by a discriminant function analysis (or CVA) using CVAGen6-IMP. A Canonical Variates Analysis assesses the ability to correctly classify random, individual specimens in a dataset to groups (e.g. male or female), rather than asking if the two groups merely have a different shape. This program feature is crucial in determining the power or robusticity of the predictive power from a certain morphological feature. The program computes partial warp scores to a common reference, and determines how many CVA axes there are in the data at a p=0.05 level of significance and computes the canonical variate scores of all specimens entered (Sheets 2001).

CVAGen6 generates a plot signifying the similarities or differences in "clusters" of landmarks from specimens of different groups. Groups of specimens may either be tightly clustered together and distinct from one another when observing the CVA plot, or be dispersed exhibiting homogeneity. This clustering or dispersal is indicative of variation between groups. The program then generates a Canonical Variates Analysis-plot that shows whether any superimposition or overlay is present in the clusters of landmarks.

- **TwoGroup6:**

Determination of how each group "assembled" in a cluster of landmarks was performed using TwoGroup-program-IMP TwoGroup6. Then inter-group shape differences between the males and females were tested by these means. TwoGroup uses BC files to perform two-group comparisons in a sample population. The amount of overlap can be scrutinized to establish whether any variations are seen.

This program also uses Hotelling's T^2-test and Goodall's F-test to calculate p-values to determine the statistical significance, if any, of the morphological feature analyzed. Goodall's F-test specifically compares the Procrustes distance between the means of two samples to the amount of variation found in the samples (Scholtz 2006).

To test for intra-observer repeatability, 15 male specimens and 15 female specimens were randomly selected and re-assigned the above-described homologous landmarks for each of the four views of the humerus and os coxae. The repeated landmark data was statistically compared to the original data set using Hotelling's T^2-test and Goodall's' F-test of the TwoGroup program.

To test for inter-observer repeatability, the four views of the same 30 specimens were once again selected and an independent observer re-assigned the defined landmarks. The independent observer was someone not involved in the study, but who had experience with geometric morphometrics. The landmark data assigned by the observer was once again statistically compared to the original dataset using Hotelling's T^2-test and Goodall's F-test of the TwoGroup program.

Table 3.1: Frequency distribution of males and females in total sample size (N = 593).

Group	Male	Female
50 years old or younger("young")	151	79
Over 50 years old ("old")	253	110
Total	404	189

Table 3.2: Non-metric distal humerus characteristics for males and females.

Feature	Male	Female
Olecranon fossa shape:	The fossa appears roughly triangular	The fossa appears oval
Angle of the medial epicondyle:	The medial epicondyle extends parallel to the table (or exhibits a slight angle) placed posterior side up	The medial epicondyle clearly angles upwards away from the parallel plane of the tabletop surface when placed posterior side up
Medial epicondylar symmetry:	Medial epicondyle sits within the trochlear profile with an equal amount of trochlear bone surrounding it. Appears "symmetrical"	Medial epicondyle sits towards the posterior portion of the trochlear profile, creating asymmetry in the trochlear bone surrounding it
Trochlear extension:	Medial edge of the trochlea extends further distally than does the lateral edge	Distal extension of the medial and lateral edges of the female trochlea is almost equal; more symmetrical in shape

Table 3.3: Non-metric pelvic characteristics for males and females.

Feature	Male	Female
Length of subpubic concavity:	Short, stout curving surface with little to no distance between inferior of the pubic symphysis and beginning margin of the ischial surface	Laterally curving surface of some distance inferior to the pubic symphysis
Width of the subpubic angle:	Short and narrow, less than 90 degrees	Wide, flared and extended past a 90-degree angle
Width of the ischio-pubic ramus:	Thick and broad	Thin and narrow
Width of the greater sciatic notch:	Narrow, relatively short	Broad and wide-angled

Table 3.4: Descriptions of measurements taken on postcranial elements.

From:* Data Collection Procedures for Forensic Skeletal Material, *Moore-Jansen et al., 1994

Long bone	Measurement	Description
Humerus:	Maximum vertical diameter, head of the humerus	The direct distance between the most superior and inferior points on the border of the articular surface
	Maximum diameter of the humerus at midshaft	Measure of the midpoint of the humerus located a few millimetres below the inferior margin of the deltoid tuberosity
	Epicondylar breadth of the humerus	The distance of the most laterally protruding point on the lateral epicondyle from the corresponding projection of the medial epicondyle
	Midshaft circumference of the humerus	Circumference measurement at the same position as maximum diameter
Ulna:	Superior transverse diameter of the head of the ulna	Maximum diameter of the superior ulnar head, from the lateral margin to the outermost edge of the projection above the semilunar notch
	Medial transverse diameter of the head of the ulna	Maximum diameter of the ulnar head, from the deepest point of the semilunar notch to the deepest point on the surface of the coronoid process
	Inferior transverse diameter of the head of the ulna	Maximum diameter from the inferior margin of the radial notch to the most inferior margin of the coronoid process
	Maximum diameter of the ulna at midshaft	Maximum diameter of the ulnar diaphysis where the crest exhibits the greatest development
	Maximum distal diameter of the ulna	Maximum diameter measured along the inferior border, superior to the styloid process
	Olecranon-coronoid distance	Maximum distance from the most superior point of the anterior projection of the olecranon process to the anterior projection of the coronoid process
Radius:	Maximum diameter of the head of the radius	Maximum diameter of the circular head of the radius
	Maximum diameter of the radius at midshaft	Maximum diameter, whether measured in the sagittal plane or transversely
	Maximum distal diameter of the radius	Maximum diameter from the outermost projection of the styloid process to the outermost projection of the ulnar notch
Femur:	Maximum vertical diameter of the femoral head	Maximum diameter measured superior-to-inferior on the border of the articular surface
	Maximum diameter of the femur at midshaft	The maximum diameter, usually found as the anterio-posterior position, measured approximately at the midpoint of the diaphysis, at the highest elevation of the linea aspera. May be located at the medio-lateral margin
	Epicondylar breadth of the femur	The distance between the two most laterally projecting points on the epicondyles
	Circumference of the femur at midshaft	Circumference measured at the midshaft, same level of the sagittal and transverse diameters

Table 3.4 (continued)

Long bone	Measurement	Description
Tibia:	Maximum bicondylar breadth of the proximal tibia	The maximum distance between the two most laterally projecting points on the medial and lateral condyles of the proximal epiphysis
	Maximum diameter of the tibia at midshaft	The distance between the anterior crest and the posterior surface at the level of the nutrient foramen
	Maximum epiphyseal breadth of the distal tibia	The distance between the most medial point on the medial malleolus and the lateral surface of the distal epiphysis
Fibula:	Maximum diameter of the proximal fibula	The distance between the most lateral edge and most medial edge of the proximal epiphysis
	Maximum diameter of the fibula at midshaft	The maximum diameter at the midshaft, usually including the superior interosseous crest
	Maximum diameter of the distal fibula	The distance between the most lateral edge and the most medial edge of the distal epiphysis, usually including the edge of the lateral malleolus
Pelvis:	Maximum length of the pelvic bone	The distance between the top margin of the iliac crest and the margin of the pubic symphysis
	Maximum width of the pelvic bone	The distance between the medial and lateral edges of the iliac blades
	Ischio-pubic index	Pubis length x 100/ Ischium length. Pubis length is measured by placing spreading callipers on the superior tip of the pubic symphysis and the meeting point of the ischium and pubis within the acetabulum. This meeting point is visualized as an irregularity, a change in thickness of the bone, or a notch. Ischium length is measured by placing spreading callipers on the most inferior point of the ischial tuberosity to the convergence point within the acetabulum

Figure 3.1: Triangular olecranon fossa shape observed in males.

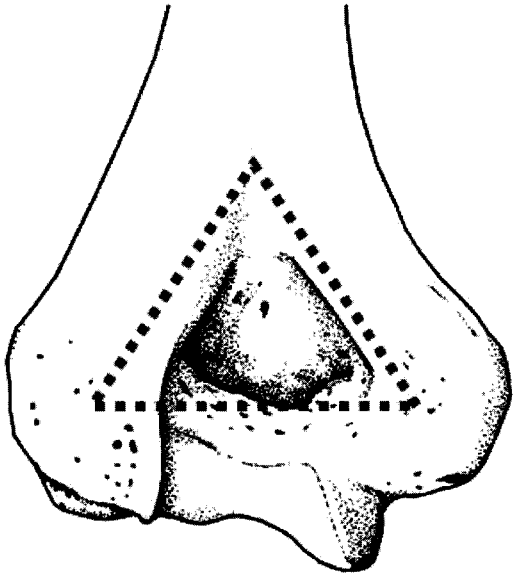

Figure 3.2: Oval olecranon fossa shape observed in females.

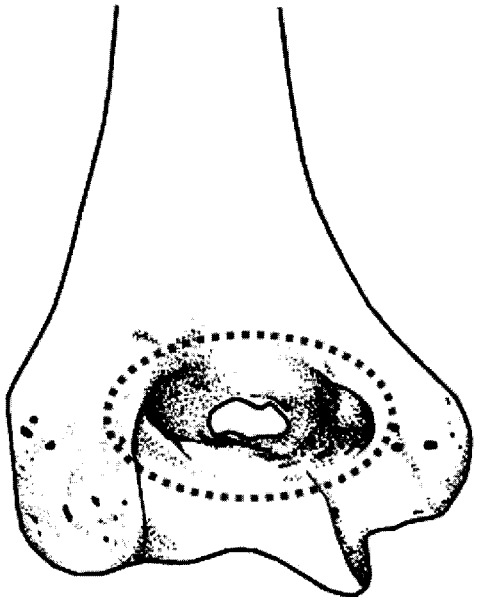

Figure 3.3: Angle of the medial epicondyle observed in males (humerus is posterior side up). The angle appears parallel to the table on which the humerus rests.

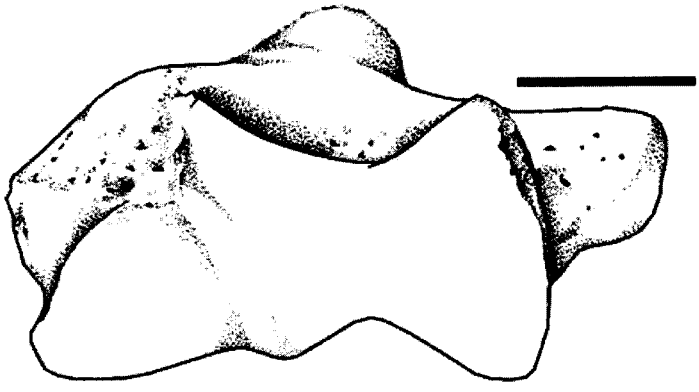

Figure 3.4: Angle of the medial epicondyle observed in females. The angle appears to project upwards from the table on which the humerus rests.

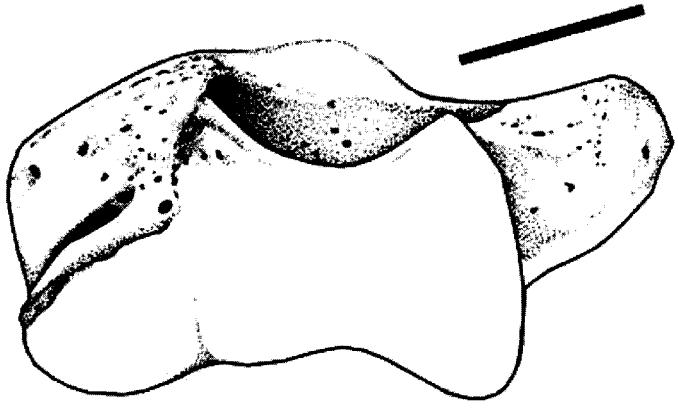

Figure 3.5: Medial epicondylar symmetry observed in males. The medial epicondyle sits centrally within the profile of the trochlea. Anterior surface is to the right.

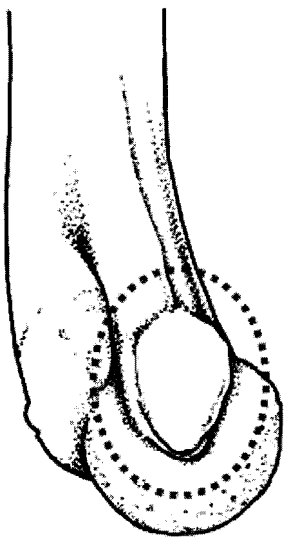

Figure 3.6: Medial epicondylar symmetry observed in females. The medial epicondyle sits posteriorly within the profile of the trochlea. Anterior surface is to the right.

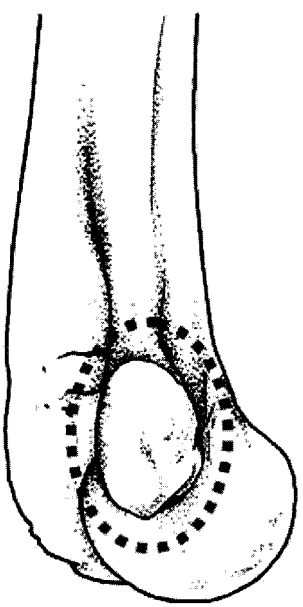

Figure 3.7: Trochlear extension observed in males. The trochlea extends well past the margin of the capitulum.

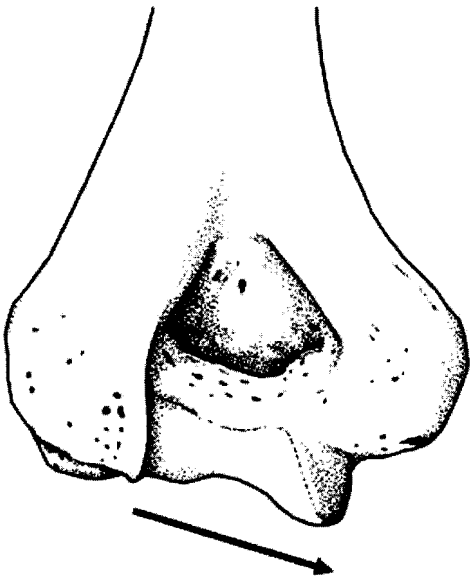

Figure 3.8: Trochlear extension/ relative symmetry observed in females. The trochlea is more symmetrical with the margin of the capitulum.

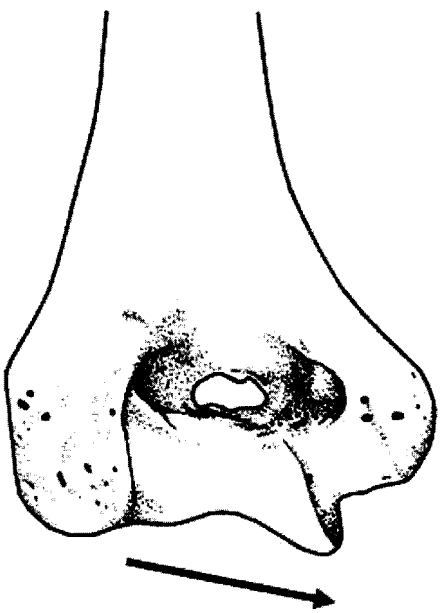

Figure 3.9: Length of the subpubic concavity as observed in males. The subpubic cavity has a short, stout curving surface.

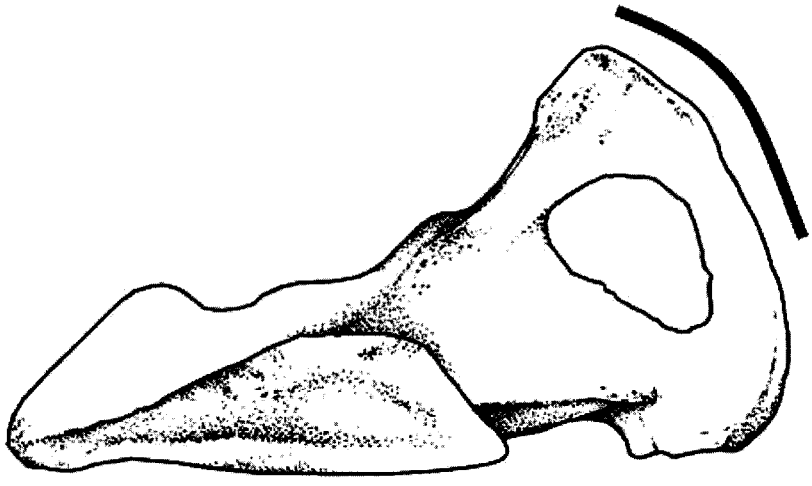

Figure 3.10: Length of the subpubic concavity as observed in females. The subpubic concavity has a long, rectangular-shaped curving surface.

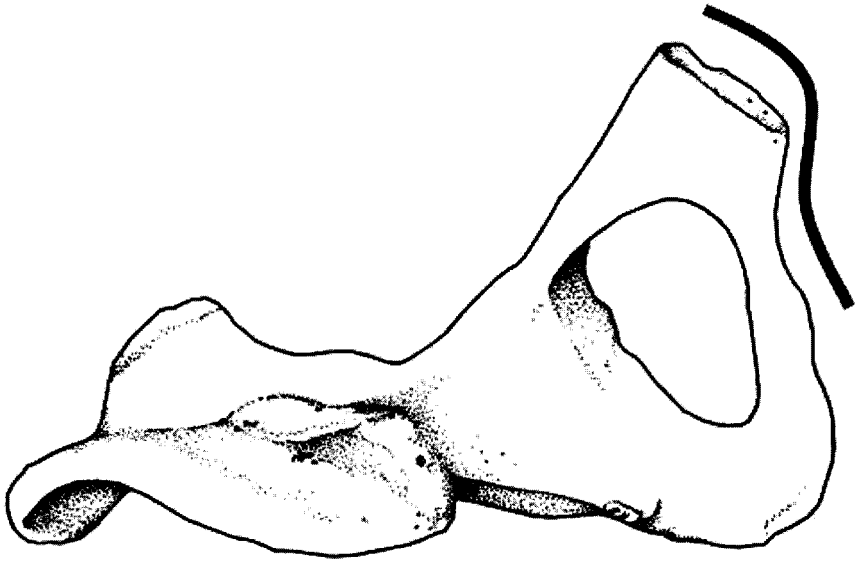

Figure 3.11: Width of the subpubic angle as seen in males. The subpubic angle is narrow.

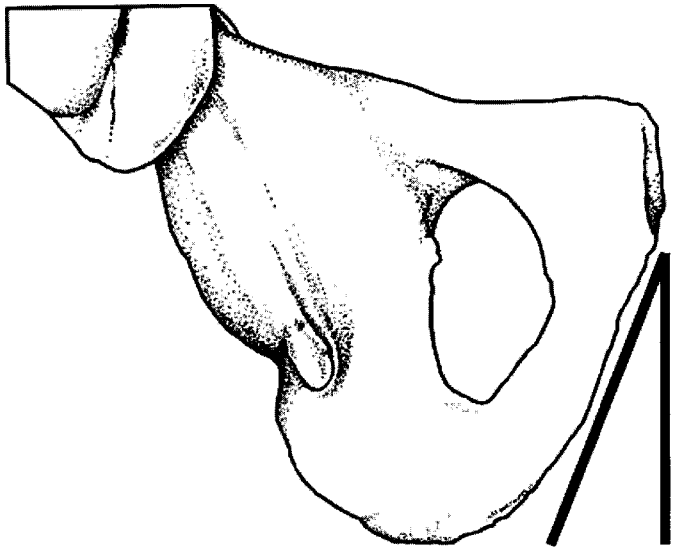

Figure 3.12: Width of the subpubic angle as seen in females. The subpubic angle is wide.

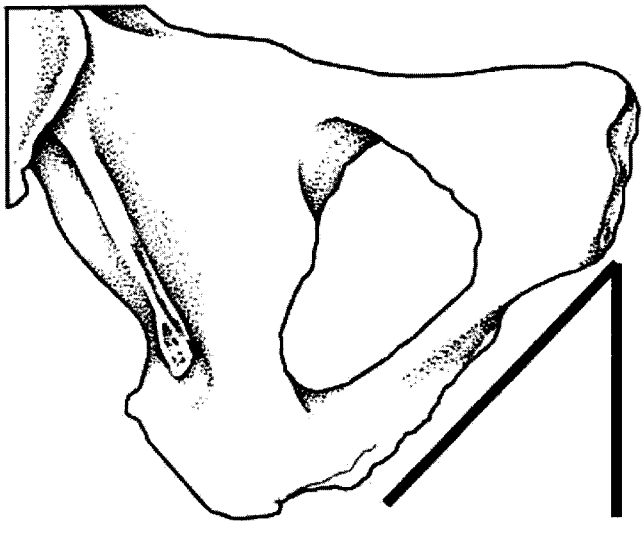

Figure 3.13: Ischiopubic ramus width as seen in males. The ramus width appears thick and broad.

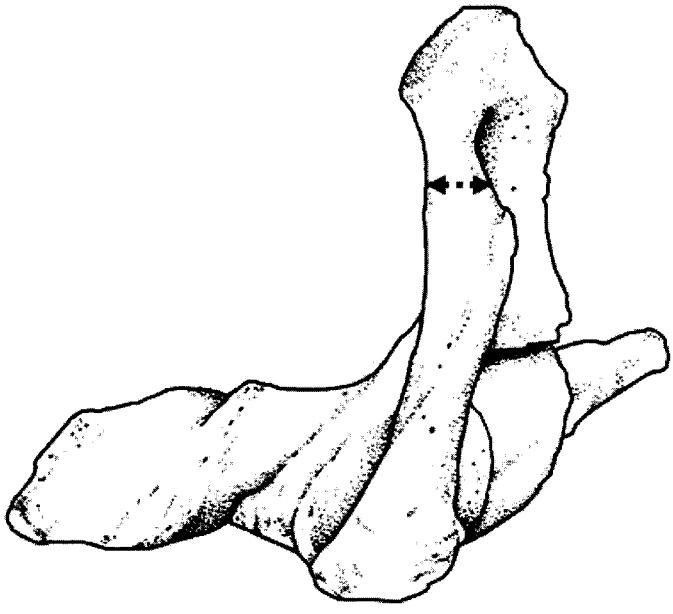

Figure 3.14: Ischiopubic ramus width as seen in females. The ramus width appears thin and gracile.

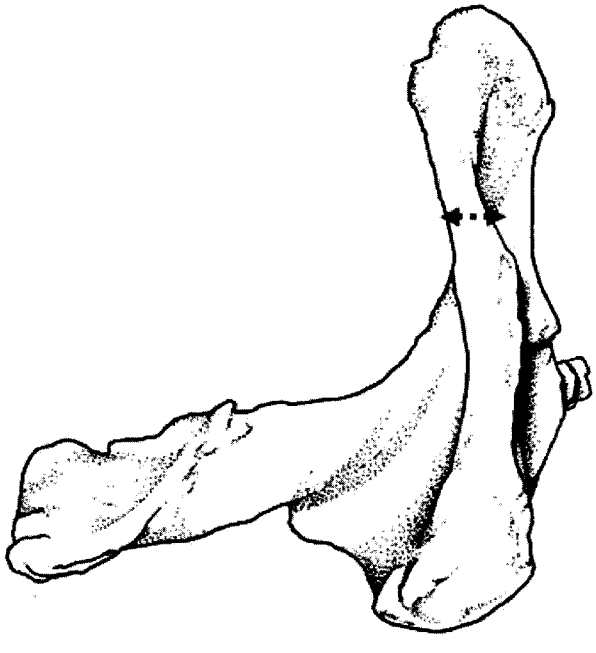

Figure 3.15: Greater sciatic notch width as seen in males. The greater sciatic notch appears narrow and compacted.

Figure 3.16: Greater sciatic notch width as seen in females. The greater sciatic notch appears wide and expansive.

Figure 3.17: Measurements of the humerus. a) maximum vertical diameter of the humeral head, b) maximum midshaft diameter, c) distal epicondylar breadth of the humerus.

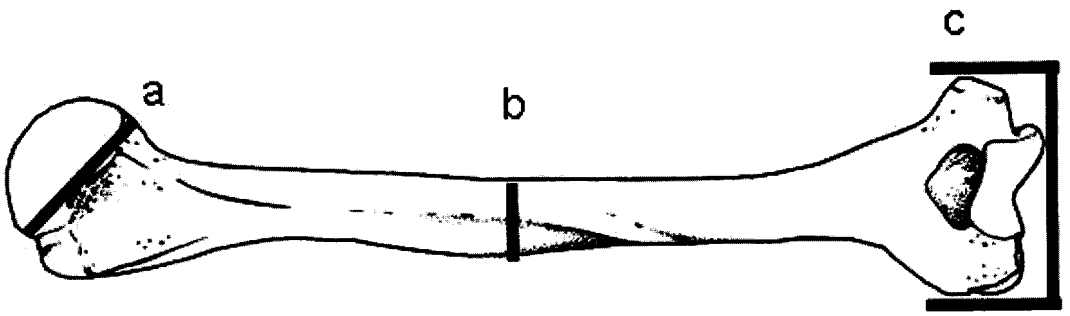

Figure 3.18: Measurements of the ulna. a) maximum superior ulnar head diameter, b) maximum medial ulnar head diameter, c) maximum inferior ulnar head diameter, d) maximum midshaft diameter, e) maximum distal diameter.

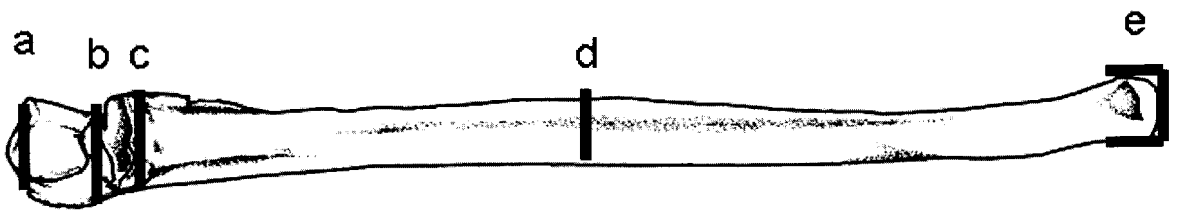

Figure 3.19: Measurements of the radius. a) maximum vertical diameter of the radial head, b) maximum midshaft diameter, c) distal breadth of the radius.

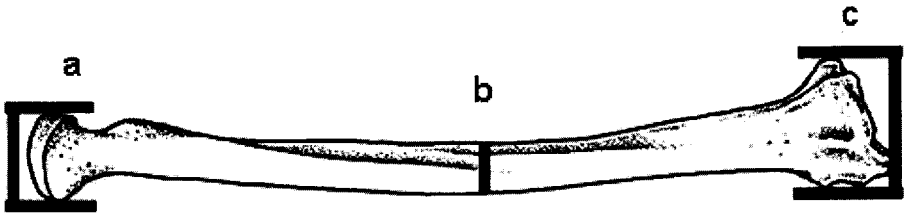

Figure 3.20: Measurements of the femur. a) maximum vertical diameter of the femoral head, b) maximum midshaft diameter, c) distal epicondylar breadth of the femur.

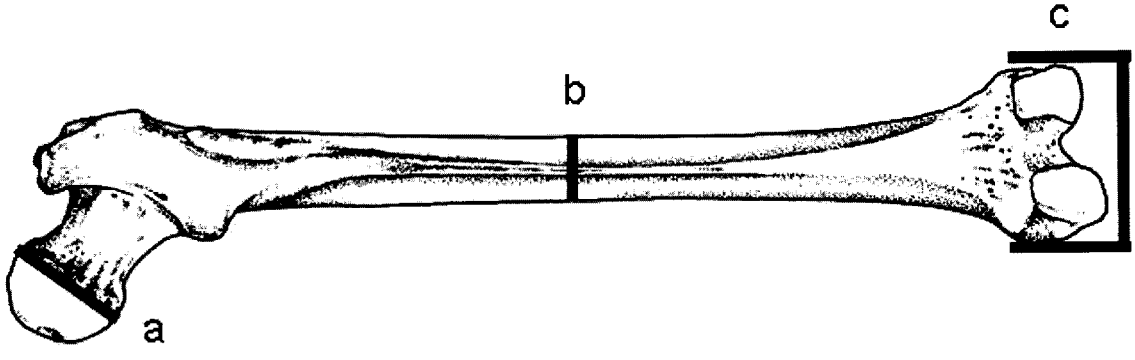

Figure 3.21: Measurements of the tibia. a) maximum bicondylar breadth of the tibia, b) maximum midshaft diameter, c) distal breadth of the tibia.

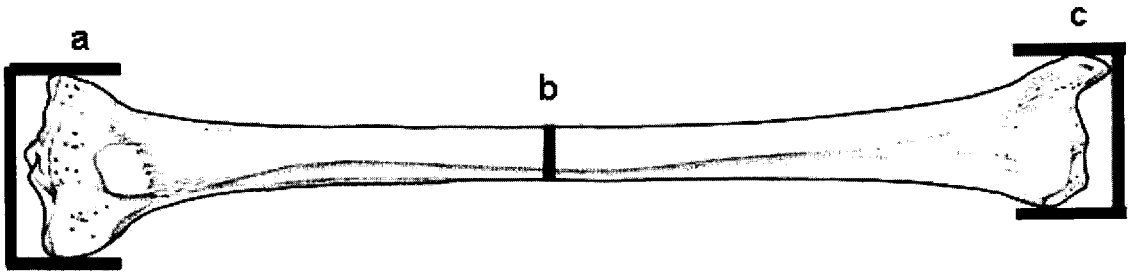

Figure 3.22: Measurements of the fibula. a) maximum diameter of the proximal fibula, b) maximum midshaft diameter, c) distal breadth of the fibula.

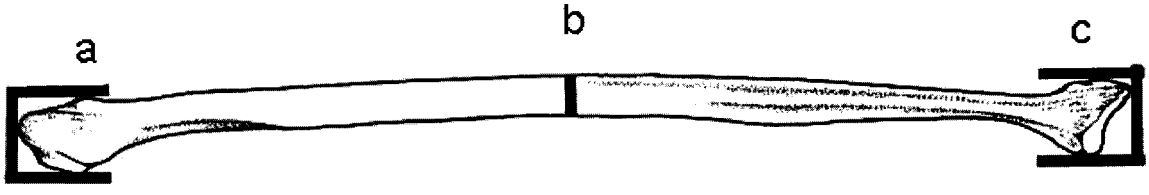

Figure 3.23: Measurements of the pelvis. a) maximum length, b) maximum breadth.

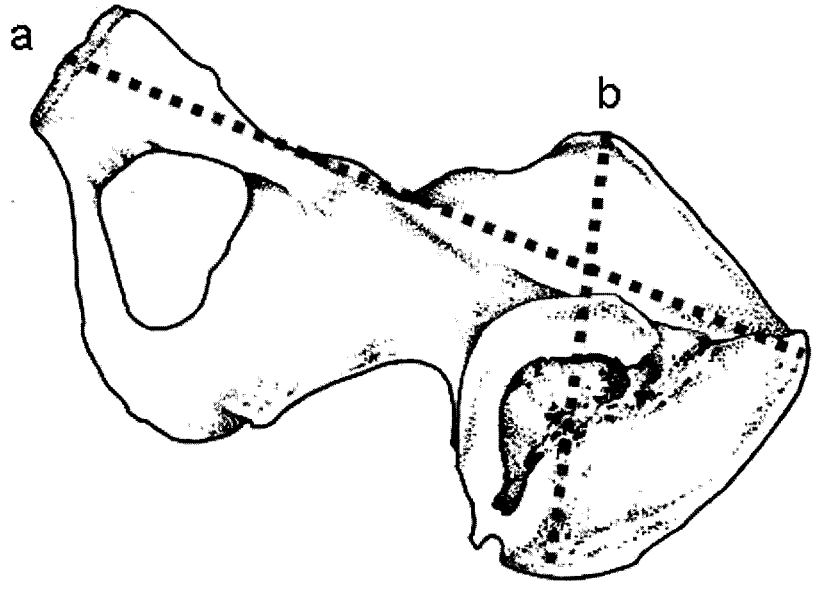

Figure 3.24: Measurements used to calculate the ischio-pubic index. a) pubis length, b) ischium length.

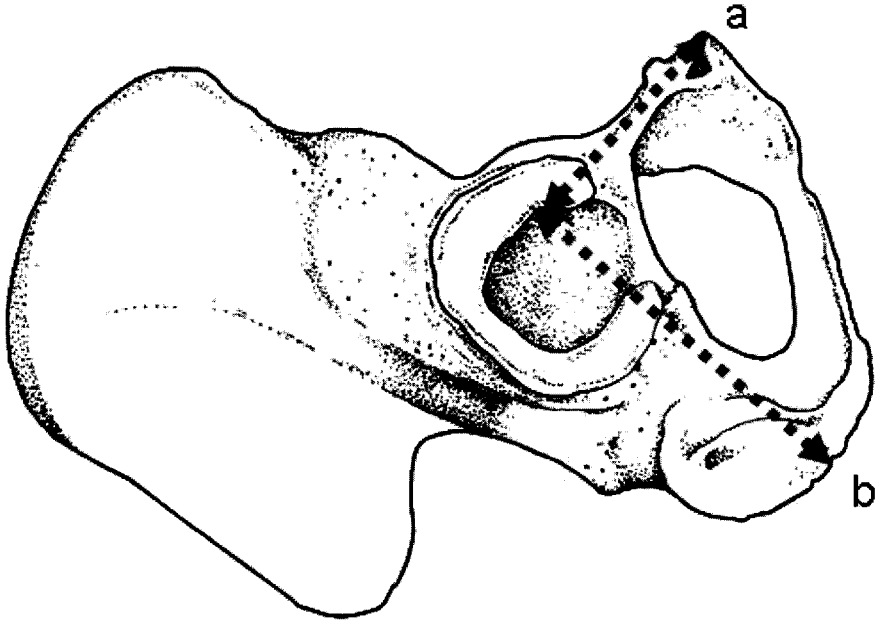

Figure 3.25: Homologous landmarks for the EPI view. See description of each landmark location in Section 3.4.1.

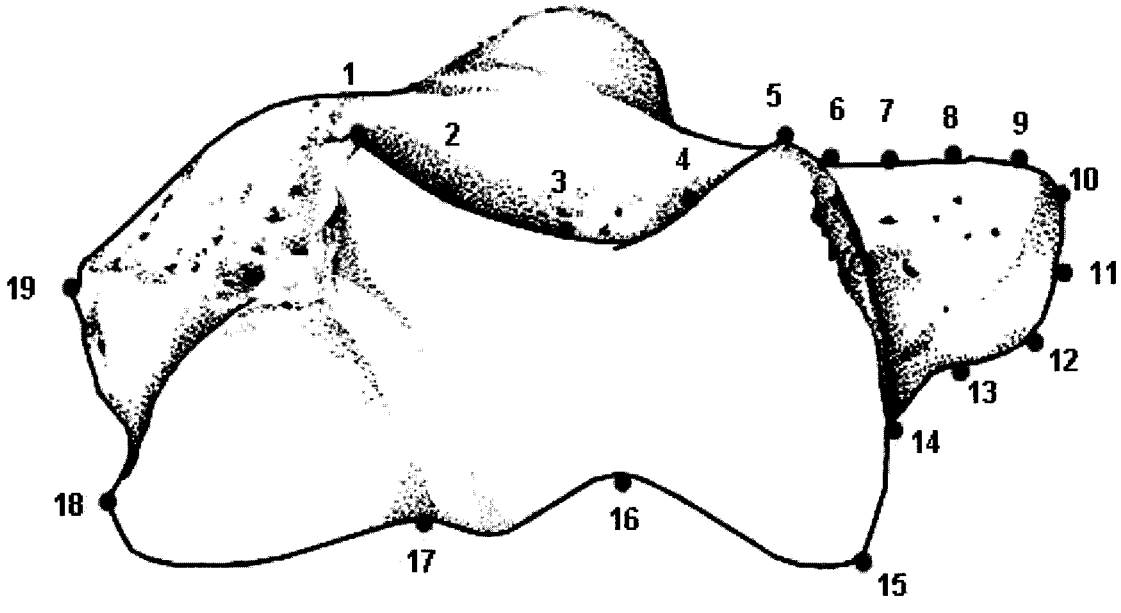

Figure 3.26: Homologous landmarks for the view OL. See description of each landmark location in Section 3.4.2.

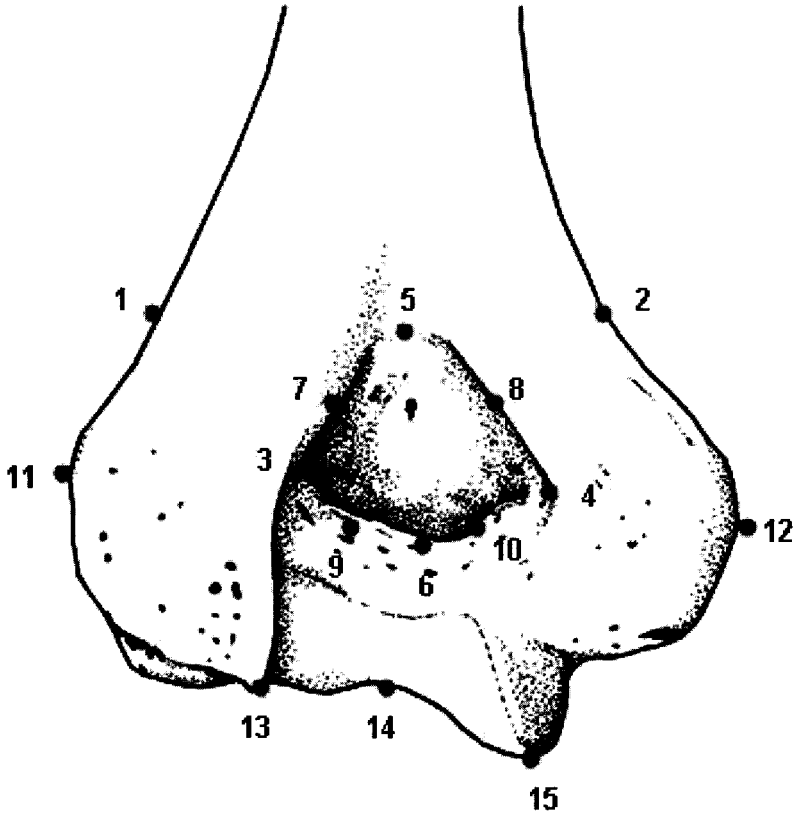

Figure 3.27: Homologous landmarks for the view SUB. See description of each landmark location in Section 3.4.3.

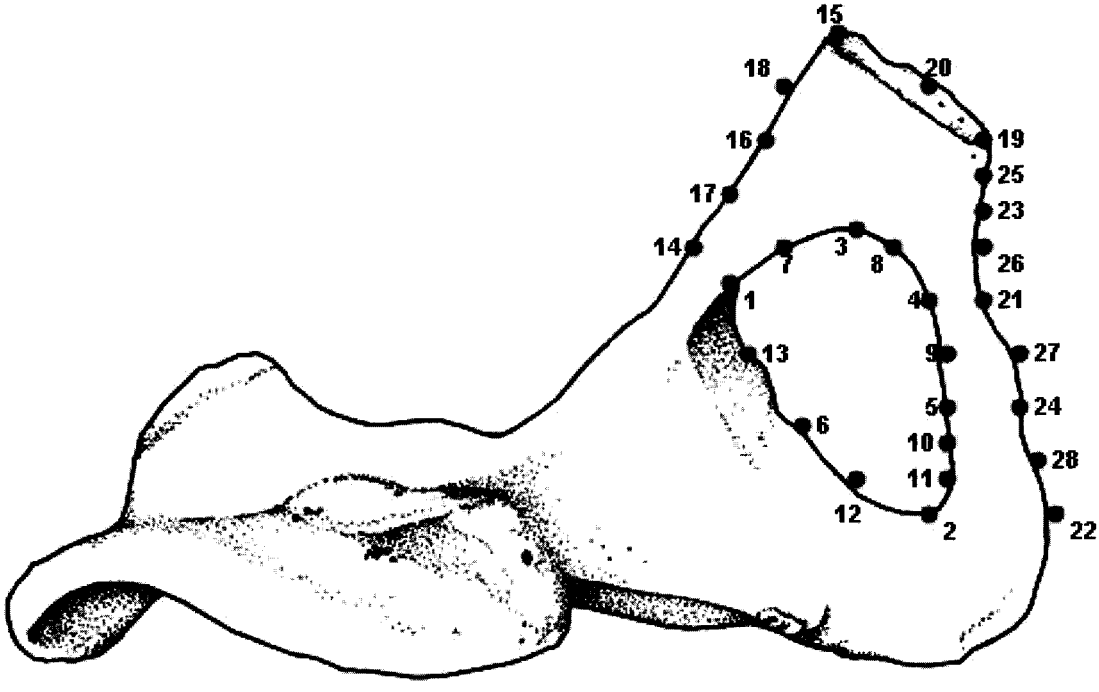

Figure 3.28: Homologous landmarks for the view SCI. See description of each landmark location in Section 3.4.4.